EPRI | ELECTRIC POWER RESEARCH INSTITUTE

Radiofrequency Burns in the Workplace

Radiofrequency Burns in the Workplace

1015627

Final Report, November 2008

EPRI Project Manager
R. Kavet
M. Silva

ELECTRIC POWER RESEARCH INSTITUTE
3420 Hillview Avenue, Palo Alto, California 94304-1338 • PO Box 10412, Palo Alto, California 94303-0813 • USA
800.313.3774 • 650.855.2121 • askepri@epri.com • www.epri.com

DISCLAIMER OF WARRANTIES AND LIMITATION OF LIABILITIES

ORGANIZATION(S) THAT PREPARED THIS DOCUMENT

Washington State University

Richard Tell Associates, Inc.

EPRI

NOTE

For further information about EPRI, call the EPRI Customer Assistance Center at 800.313.3774 or e-mail askepri@epri.com.

CITATIONS

This report was prepared by

Washington State University
Dana Hall 145
Pullman, WA 99164-2713

Principal Investigators
R. Olsen
J. Schneider

Richard Tell Associates, Inc.
1872 E. Hawthorne Ave.
Colville, WA 99114-9352

Principal Investigator
R. Tell

This report describes research sponsored by EPRI.

The report is a corporate document that should be cited in the literature in the following manner:

Radiofrequency Burns in the Workplace. EPRI, Palo Alto, CA: 2008. 1015627.

PRODUCT DESCRIPTION

Radiofrequency (RF) burns are the result of localized and intense heating of skin and, in some cases, underlying tissue, caused by the flow of RF currents. The burn may be the result of an electrical arc or RF currents associated with direct contact between the body and an RF energized conductor. RF burns can occur when high RF voltage differences exist between the body and an object sufficient to result in an arc between the object and the body. Typically, RF burns are often associated with very small electrical arcs when accidentally touching bare element antennas that are transmitting or when contacting conductive objects in strong RF field environments such as antenna tower guy wires. Empirical assessments of RF burn conditions have suggested that when the open circuit RF potential between the object and the body exceeds approximately 140 volts, RF burns may be experienced as the object and the body touch. While electromagnetic models to predict RF burns currently exist for frequencies less than 3 MHz, these same models are inadequate at higher frequencies. This study's goal was to develop electromagnetic models of both the metallic structure and the human body appropriate for higher frequencies.

Results and Findings

Analytical and numerical electromagnetic models for two important cases that are useful for predicting RF burns at higher frequencies than previously possible have been developed. The specific cases are for humans touching vertical masts and horizontal fences that are exposed to electromagnetic fields from nearby sources. Each model is supported by a theory that relates the contact current with temperature rise near the point of contact. The models can be used to determine threshold conditions for an RF burn.

Challenges and Objective(s)

In addition to developing electromagnetic models of both the metallic structure and the human body appropriate for higher frequencies, the project used these models to investigate the following questions:

- What conditions lead to RF burns?
- What conditions are conducive for RF burns while the exposure field is below the maximum permissible exposure (MPE) limits specified in appropriate standards?
- What parameters should be used to describe the potential for RF burns?
- Why is the probability of an RF burn during contact with a conducting object apparently reduced at higher frequencies?
- Is there a more basic rationale for RF contact current limits?

- Is there a rationale for setting an upper frequency beyond which contact current limits should not or need not be set? If so, what should be the upper frequency limit for contact current exposure?
- Above what frequency is it no longer permissible to ignore direct interaction of electromagnetic fields with the body and to model a human as a single impedance? What model of a human is appropriate above this frequency?

Applications, Values, and Use

The analytical and numerical electromagnetic models developed in this project can be used to determine threshold conditions for RF burns. A strategy for extending these models to higher frequencies also has been developed. The higher frequency models use the finite difference time domain (FDTD) method and incorporate an anatomically correct model for a human.

EPRI Perspective

RF burns may occur even when electromagnetic exposure fields are smaller than the MPEs listed in the most widely used national and international RF safety standards. The higher the frequency, however, the less likely RF burns will occur due to contact with objects that are not directly energized. As a corollary to this, the electromagnetic field exposure required to cause an RF burn increases at higher frequencies. While electromagnetic models to predict RF burns currently exist for lower frequencies, these same models are inadequate at higher frequencies. This project has developed new models that overcome that limitation.

Approach

The project team first clarified which aspects of RF burns require investigation. Specifically, the team discussed why arcs sometimes associated with RF burns are not considered in this study. Following this discussion, models are introduced that are used to calculate currents that lead to RF burns due to contact with parasitically and directly energized objects at frequencies higher than those allowed for in quasi-static models. These models are a person in contact with the bottom of an insulated vertical mast, a person in contact with the end of a long horizontal fence grounded at the far end, and a person in contact with a linear antenna. These models can be used to determine the limitations of quasi-static theory, to study why RF burns can occur even though the energizing field is less than MPE limits, and to ascertain why RF burns appear to occur less frequently at higher frequencies. These models, however, are limited to the case where direct interaction of the field with the body is ignored and a human can be represented by a single impedance (about 20 MHz). To resolve this limitation, the project team developed a thermal model that can be used to determine the amplitude of contact current responsible for a rapid enough temperature rise to cause an RF burn. Next, a more accurate model of the human body was incorporated into the system so that it can be studied at frequencies up to hundreds of MHz. This allows the body to interact directly with the field and to be modeled more accurately than as a single impedance. Using the FDTD method to solve this model, determining whether RF burns can occur at frequencies higher than 100 MHz is possible.

Keywords

Radio-Frequency Exposure
Radio-Frequency Burns
Occupational Safety

EXECUTIVE SUMMARY

In certain situations a person may be in contact with a metallic object and simultaneously exposed to a radio frequency (RF) electromagnetic field from a nearby source. Under some conditions, the person can experience an intense heating of his/her skin and tissue near the point of contact. When this intense heating happens, it is said that the person has experienced an RF burn. Such a burn can occur when the frequency (f) of a sinusoidally varying electromagnetic exposure field is greater than about 100 kHz (i.e., within the frequency range of RF fields) and the area of contact is small (i.e., significantly less than 1 cm^2). RF burns have been reported for human contact with vertical cables or masts near AM broadcast antennas (535 – 1710 kHz) that have relatively strong electromagnetic fields. But an RF burn can also occur with weaker fields if the object to which the person is connected is at its first resonance (e.g., a wire of length near 150/f meters where f is given in megahertz). The burn occurs because the electric current injected into the body through the point of contact has a density high enough to cause significant energy absorption and hence rapid heating of the electrically lossy skin and tissue.

RF burns can occur despite the fact that the electromagnetic exposure fields are smaller than the maximum permissible exposures (MPEs) listed in the most widely used national and international RF safety standards. The higher the frequency, however, the less likely it is that RF burns will occur due to contact with objects that are not directly energized. As a corollary to this, the electromagnetic field exposure required to cause an RF burn increases at higher frequencies. While electromagnetic models to predict RF burns currently exist for lower frequencies (i.e, less than 3 MHz), these same models are known not to be adequate at higher frequencies than this.

The purpose of this study was to develop electromagnetic models of both the metallic structure and the human body appropriate for higher frequencies as well as to use these models to answer the following questions.

- What parameters (e.g., voltage, current) should be used to describe the potential for RF burns?
- Under what conditions can RF burns occur, including those when the exposure field is below the maximum permissible exposure (MPE) limits specified in appropriate standards?
- Why is the probability of an RF burn during contact with a conducting object apparently reduced at higher frequencies?
- Is there a rationale for setting an upper frequency beyond which contact current would not cause a burn and what is that frequency?
- Above what frequency is it no longer permissible to ignore direct interaction of the electromagnetic fields with the body (i.e., the assumption that all interaction with the body

comes from the current injected at the contact point) and to model a human as a single lumped impedance element? What model of a human is appropriate above this frequency?

Analytical and numerical electromagnetic models for two important cases that are useful for predicting RF burns at higher frequencies than previously possible have been developed. The specific cases considered are for humans touching vertical masts and horizontal fences that are exposed to electromagnetic fields from nearby sources. Each model is augmented by a theory that relates the contact current with temperature rise near the point of contact. The models can be used to determine the threshold conditions for an RF burn to occur. In addition, a strategy for extending these models to even higher frequencies has been developed. The higher frequency models will utilize the Finite Difference Time Domain (FDTD) method and incorporate an anatomically correct model of a human.

The models developed in this study indicate that

- If the human impedance is assumed to be 1500 Ω and 100 mA is taken as the threshold for an RF Burn, then the threshold electric field at which an RF burn occurs from contact with a vertical mast at its first resonance (i.e., the worst case that occurs at 150/f(MHz) meters) is approximately E_o = 0.83 f(MHz) V/m.,
- The electric field required to cause an RF burn is larger than 0.83 f(MHz) V/m if the frequency is above or below the first resonance of the vertical mast,
- At frequencies below the first resonance, the probability of an RF burn is greater for contact with tall metallic objects than for short metallic objects,
- For a given electric field exposure level, the probability of an RF burn decreases with frequency at a rate of approximately 1/f(MHz),
- At frequencies below approximately 75 MHz, RF burns can occur at electromagnetic field levels significantly less than the maximum permissible exposure in the most widely used RF Safety standards
- At frequencies higher than the first resonance, contact with taller metallic objects does not result in a greater probability of RF burns than contact with shorter metallic objects.

In addition to these findings, the report surveys the historical context of the RF burn problem and contains descriptions of the difference between low frequency electrical shock and RF burns, the possibility of injury due to arcs associated with RF burns as well as heating due to energy absorption and characteristics of and mitigation methods for RF burns.

In forthcoming work, the problem of RF burns due to human contact with metallic objects and exposure to very high frequency (VHF) electromagnetic fields will be studied. Finally, the potential for RF burns from exposure to energized antennas at VHF frequencies will be investigated.

ACKNOWLEDGMENTS

The authors of this report acknowledge the support and encouragement of Dr. Rob Kavet, EPRI EMF Health Assessment and RF Safety Program Manager, Mr. Mike Silva manager of the EPRI RF Safety Program and Dr. Gabor Mezei, manager of the EPRI Occupational Health and Safety Program. In addition they would like to acknowledge the contributions of reviewers, Dr. James Stewart, Dr. David Renew and Mr. Mike Mason. The research was supported by EPRI's RF Safety and Occupational Health & Safety programs.

CONTENTS

LIST OF FIGURES

LIST OF TABLES

1
INTRODUCTION

It is well known that electric currents induced in a grounded human body by direct exposure to 50/60 Hz electric and magnetic fields typically found near electric power lines are well below levels that cause obvious (if any) effects [1] as shown in Fig. 1-1a. Of special note here is the fact that the level of induced currents in the body is limited (in part) by the physical size of the body and the fact that the currents are reasonably well dispersed throughout the body resulting in electric current densities (J) below neurostimulatory thresholds [2].

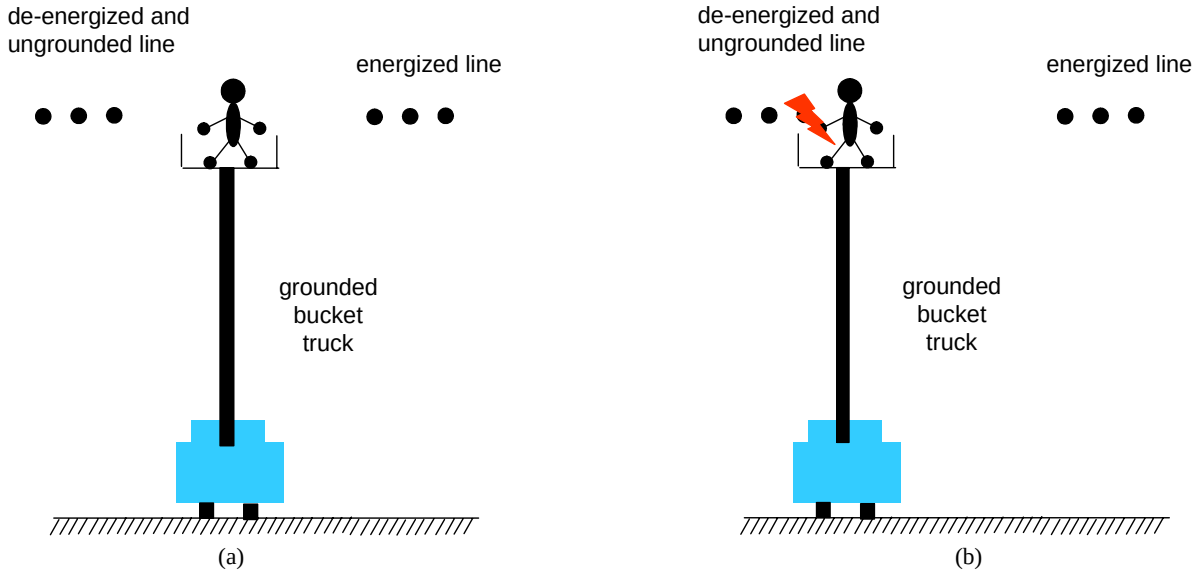

Figure 1-1
(a) Person in field near an energized line with no obvious effect. (b) Person touching a de-energized, ungrounded conductor near an energized line leading to an electrical shock[1]

The situation is different, however, if (for example) a grounded worker is in contact with a large metallic structure such as a de-energized (and ungrounded) transmission line conductor that is exposed to 50/60 Hz electric and magnetic fields from a parallel energized transmission line (Fig. 1-1b)[1]. In this case, inductive and capacitive coupling occur and obvious effects such as aversive perception or electrical shock can and do occur near the point of contact between the

[1] The authors recognize that the practice described in the text and Figure 1b is not in accord with safety practices observed by all electrical utilities. In fact, no employee would be allowed to touch the de-energized, ungrounded conductor shown in Fig. 1b without it first being appropriately grounded. The purpose of introducing this example is simply to indicate that it is a dangerous situation and to use it as an analogy to the RF burn condition to be introduced next.

body and the de-energized metallic structure [1]. These obvious effects occur for two reasons. First, the human body is "augmented" by contact with the metallic structure and this "augmented body" effectively becomes much larger than an isolated human body. The metallic structure acts like a receiving antenna that "gathers" a larger amount of energy from the electric and magnetic fields than the body would gather by itself. Second, the area of contact between the body and the structure is usually quite small and hence the electric currents traveling from the structure to the body and then to ground are concentrated in a very small cross-sectional area of tissue. This means that the electric current density (and the associated electric field E since $J = \sigma E$, where σ is the body conductivity) can be quite large in that area. Since most biological effects are related to local electric field strength in the body, it is not surprising that electrical shocks occur near these points of contact. In this context, the IEEE "basic restriction" is the limit on the local electric field strength in the body because it is a threshold most closely associated with biological effects [3].

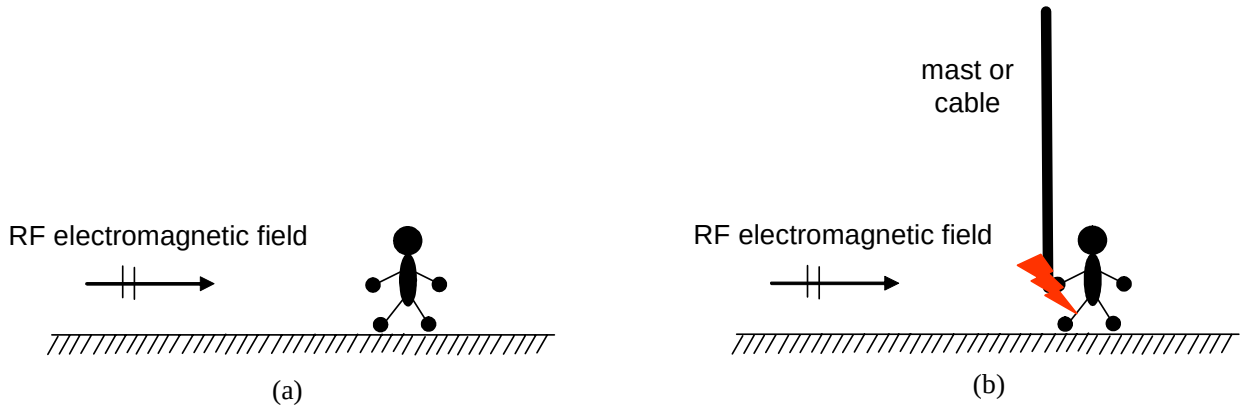

Figure 1-2
(a) Person in an RF field with no obvious effect. (b) Person touching a mast or long cable in an RF field leading to an RF burn at the point of contact.

An analogous situation occurs for human exposure to radiofrequency (RF) electromagnetic fields (3 kHz – 300 GHz) (Fig. 1-2a). Electric currents are induced in humans who are exposed to RF electromagnetic fields as shown in Fig 1-2a. However, calculations reveal that under most circumstances, currents induced by exposure fields from RF transmitters typically located near electric power lines (and the related local energy absorption rates) are below limits in relevant safety standards [4]. Further, unless the exposure field is from a very small source very close to the body, the current will be spread out over the body, resulting in a relatively small electric current density (and hence small electric field) within the body. However, RF burns can occur at points of contact between the human body and metallic structures that are exposed to electromagnetic fields from nearby sources of RF fields [5,6] as illustrated in Fig. 1-2b. This happens because the body is now "part" of a larger object and it can be said that the body is "augmented" in size. As a result, the current induced in the body may be significantly increased. As with the extremely low frequency (ELF) case described above, the connection between the body and the object often has a small area and the current injected into the body is concentrated near this point. This can result in a current density in this part of the body strong enough to raise the local temperature and cause deep burns. It is these RF burns that are the subject of this report. Given that temperature rise is what causes the burns; the "basic restriction" exposure limit is different in this case from that for exposure to ELF fields. More specifically, the basic

restriction is the specific absorption rate (SAR) that is defined as the energy absorption rate in tissue per unit mass. In terms of more fundamental variables, the SAR at a point within the body is defined as

$$SAR = \frac{J^2}{\sigma d} = \frac{\sigma E^2}{d} \; watts$$

Eq. 1-1

where J is the current density, E is the electric field, σ is the local electrical tissue conductivity and d is the tissue density. SI units are assumed.

2
DIFFERENCE BETWEEN 50/60 HZ ELECTRICAL SHOCKS AND RF BURNS

The driving force behind both 50/60 Hz electrical shocks and RF burns is the electric field and/or electric current density induced inside the body. One major difference between the two phenomena is that the physiological response to 50/60 Hz currents is not the same as that due to RF currents. This is apparent from the graph of perception and tolerance thresholds for sinusoidal electric currents shown in Fig. 2-1 [7,8]. At frequencies below approximately 10 kHz, the nerves in the body are excited by the current resulting in electrical shock. As the frequency is increased, the nerves become less sensitive to these currents in a roughly linear fashion. At frequencies above 100 kHz, the heat generated by the current flowing in the body can produce a physiological response (i.e., the sensation of heat). Electromagnetic energy is absorbed at a rate proportional to the square of the current density, which in turn causes a local temperature rise in the body. As frequency increases, this thermal response becomes essentially independent of frequency as shown in Fig. 2-1. Another difference between ELF and RF dosimetry is the dissimilar current distribution in the body due to "skin effect," which causes the electric current at higher frequencies to flow closer to the outer surface of the body rather than uniformly through the body's cross-section [9].

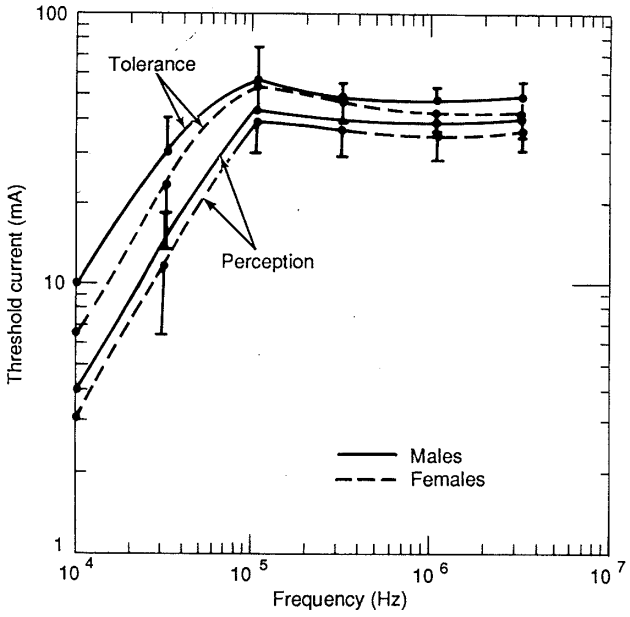

Figure 2-1
Physiological response of humans to sinusoidal electric current [7,8].
(Figure used with permission of Pat Reilly).

3
HISTORICAL BACKGROUND

A good review of the important aspects of RF exposure to electric and magnetic fields can be found on the website of the Occupational Health and Safety Administration (OSHA), United States Department of Labor [10]. On this site, it is noted that,

> Electric and magnetic fields are complex physical agents whose potential health effects are the subject of much research. Particularly controversial are the biophysical mechanisms by which these RF fields may affect biological systems. General health effects reviews explore possible carcinogenic, reproductive and neurological effects. Health effects by exposure source are noted in radar traffic devices, wireless communications with cellular phones, radio transmission, and magnetic resonance imaging (MRI).

OSHA materials relate mostly to non-ionizing, non-contact, RF exposure that dramatically reduces in power density as you move away from the source of RF energy, such as communications antennas. These "isolated humans" do not have physical contact with RF conducting devices. However, the subject of RF burns, as a result of contact with, or being in close proximity to, an RF energized circuit, such as a communications antenna, and/or a large metallic object with induced RF, is only covered briefly in the OSHA guidelines. An example of RF current induced into a mast is illustrated in Figure 1-2b. Two specific problems discussed in the OSHA document are worker contact with crane cables located near an AM broadcast antenna and worker contact with radio frequency antennas. As noted above, these cases are fundamentally different from the case for exposure of an isolated human body to RF electromagnetic fields and the exposure from contact that leads to burns is not as well understood.

Concern about occupational hazards from RF burns spawned a significant amount of research on the subject in the 1980's [5]. As mentioned above, the problems included human contact with metallic objects that are insulated from the ground and located near AM broadcast stations or high powered communication and radar antennas. In some of the early work, Ghandi and Chatterjee [6] used quasi-static theory identical to that used by power engineering researchers to study electrical shock hazard. They calculated the amount of RF current induced in a person by contact with an insulated metallic object such as a vehicle when exposed to an RF electromagnetic field. Since quasi-static theory assumes that all objects are small compared to a wavelength, the studies were limited to frequencies below approximately 3 MHz. It is interesting to note that the authors concluded, "…..there may be situations where the thresholds of perception and let-go can be exceeded for fields considerably lower than the American National Standards Institute (ANSI) recommended guideline of 615 V/m." Additional work was done by Chatterjee, Wu and Ghandi to determine a range of human body impedances useful for predicting RF burn thresholds at these frequencies [8]. For finger contact, they found impedances that ranged from roughly 1000 to 2000 ohms depending upon frequency and size of

the person. At the same time, the Navy conducted work to study the safety of their personnel who were working on ships that had communication or radar antennas that radiated high powers. The Navy summarized this research as follows [11].

> The specific level at which contact with RF voltage should be classified as an RF burn hazard is not distinct. Hazardous RF voltage is defined as the voltage that will cause a person pain or visible skin damage, or will cause an involuntary reaction. The term "hazard" does not include the lower voltages that cause annoyance, a stinging sensation, or moderate heating of the skin. Naval Sea Systems Command (NAVSEA) Code 62E, has established that an open-circuit RF voltage exceeding 140 volts on an item in an RF radiation field is to be considered hazardous. However, field tests have shown that because of the many variables involved, it is not uncommon to encounter significantly higher voltages that do not result in a burn problem.

This work led to a suggested limit on contact voltage in the IEEE Standard for exposure to RF Electromagnetic Fields [12]. Specifically, the standard states that for frequencies between 100 kHz and 100 MHz, the maximum allowable open circuit voltage measured between any two points of contact with the body is 140 volts (rms).

Although open circuit voltage is an important measure of the probability for an RF burn and is relatively easy to measure, it is contact current through the body that can be directly related to RF burns. To calculate contact current from open circuit voltage, it is necessary to know both the human body impedance described above as well as the system impedance (later called a Thevenin impedance) that depends upon the frequency and the specific geometry of the system that the person is contacting.

Given that contact current is more closely related to RF burns, standards have been written by the IEEE and the International Commission on Non-Ionizing Radiation Protection (ICNIRP) for human exposure to RF contact currents [12, 13]. It is useful to note that, at this time, the Federal Communication Commission (FCC) standard does not have a limit for contact current. For “touch” exposure to sinusoidal currents at frequencies between 100 kHz and 110 MHz, the ICNIRP guidelines specify a maximum contact current of 20 mA and 40 mA for general public and occupational exposures respectively. The limits in the IEEE Standard for the same situations are 16.7 mA and 50 mA, but an averaging time of 6 minutes is allowed. There are no standards for frequencies above 110 MHz

The upper frequency for the contact current limit was not selected using a scientifically based rationale. In fact, according to the ICNIRP guidelines, “the upper frequency for contact current is imposed by lack of data on higher frequencies rather than by the absence of effects.” One example of an RF burn that can occur at frequencies above 110 MHz is found in [14] and it has been suggested in that paper that contact current limits be extended to higher frequencies. One purpose for this study is to develop a rational basis for evaluating the potential for RF burns at frequencies greater than 110 MHz that might lead to a different upper frequency limit.

4
RESEARCH QUESTIONS

There are now several important research questions that are addressed in this report.

- What parameters (e.g., voltage, current) should be used to describe the potential for RF burns?
- What are the conditions for which RF burns can occur?
- What are the conditions for which RF burns can occur while the exposure field is below the maximum permissible exposure (MPE) limits specified in appropriate standards?
- Is there a more basic rationale for RF contact current limits?
- Why is the probability of an RF burn during contact with a conducting object apparently reduced at higher frequencies?
- Is there a rationale for setting an upper frequency beyond which contact current limits should not or need not be set?
- If so, what should be the upper frequency limit for contact current exposure?
- Above what frequency is it no longer permissible to ignore direct interaction of the electromagnetic fields with the body (i.e., the assumption that all interaction with the body comes from the current injected at the contact point) and to model a human as a single impedance? What model of a human is appropriate above this frequency?

The purpose of this report is to answer the questions listed above.

5
REPORT ORGANIZATION

The results of the study are presented as follows. First, a clarification is made about what aspects of RF burns are studied and which are not. More specifically, the question of why arcs sometimes associated with RF burns will not be considered here is discussed. Following this, models that can be used to calculate currents (that lead to RF burns) due to contact with parasitically and directly energized objects at frequencies higher than those allowed for quasi-static models will be introduced. These are respectively, a person in contact with the bottom of an insulated vertical mast, a person in contact with the end of a long horizontal fence grounded at the far end and a person in contact with a linear antenna. These models can be used to determine the limitations of quasi-static theory, to study why RF burns can occur despite the fact that (for the parasitic case) the energizing field is less than MPE limits and why RF burns appear to occur less frequently at higher frequencies. But, they are limited to the case for which direct interaction of the field with the body is ignored and a human can be represented by a single impedance (i.e., about 20 MHz). Then, a thermal model is developed that can be used to determine the amplitude of contact current responsible for a rapid enough temperature rise to cause an RF burn. This may be useful for identifying a different rationale (i.e., basic restriction) for the exposure limit on RF contact current. In the next section, a more accurate model of the human body is incorporated into the system that will allow the aforementioned system to be studied at frequencies up to hundreds of MHz. This will both allow the body to interact directly with the field and to be modeled more accurately than as a single impedance. The model will be solved using the Finite Difference Time Domain (FDTD) method. Using this model it will be possible to examine whether RF burns can occur at frequencies higher than 100 MHz.

6
ARC DAMAGE VS. HEATING DAMAGE

If a charge-free conducting object is immersed in a 50/60 Hz electric field, it acquires a constant electrical potential with respect to ground equal to the unperturbed space potential at its center. As it is moved close to a conductor held at "ground" potential, the electric field between the two conductors increases. Eventually, this electric field may be large enough (assuming that there is enough charge available) to cause an arc. This is similar to the electrostatic discharge between a fingertip and a doorknob shown in Fig. 6-1. When enough charge has been transferred and the voltage between the two conductors is too small to sustain the arc, the arc is extinguished [1]. This initial "arc" (i.e., a "transient" current) is of very short duration. For the "electrostatic" case shown in Fig. 6-1, the event ends after this transient. However, if contact is made with an object exposed to 50/60 Hz fields, a current continues to flow back and forth between the two conductors since the electric field surrounding them is constantly oscillating and the charge distribution required to keep them at ground potential changes. This current is the "steady state" current between the two conductors [1].

Figure 6-1
Finger-doorknob electrostatic arc discharge due to carpet charging.

By analogy, there also may be an arc followed by a steady state current when a human in contact with or very close to the ground comes into contact with an insulated structure immersed in an RF electromagnetic field [15]. As the human's finger comes close to an insulated metallic object, there is an increasingly large electric field between the finger and the object as shown in Fig 6-2a. If this field is high enough and there is enough current available, the air breaks down and one or more arcs can be created between the finger and the object before contact occurs as

shown in Fig 6-2b. It is, in principle, possible that this arc could be perceived by and/or cause damage to the finger. But, this incident is usually brief because (in most cases) the finger is moving towards the object relatively rapidly. Due to the brevity of the period during which the arc could occur as well as the difficulty in describing such an arc, direct damage from the arc will not be considered here except for one possible effect. It is possible that the arc could puncture the skin and (since the skin has high resistance) create a small area (of size equal to that of the arc area) of relatively low contact resistance between the metallic object and the body. This might reduce the total body impedance and restrict the current to a small region of the finger. The importance of such a small area is that it would create a very high current density very close to the current entry point. This high current density, in turn, creates a very high specific absorption rate (SAR) that can cause a rapid temperature rise in the finger as shown in Fig. 6-2c.

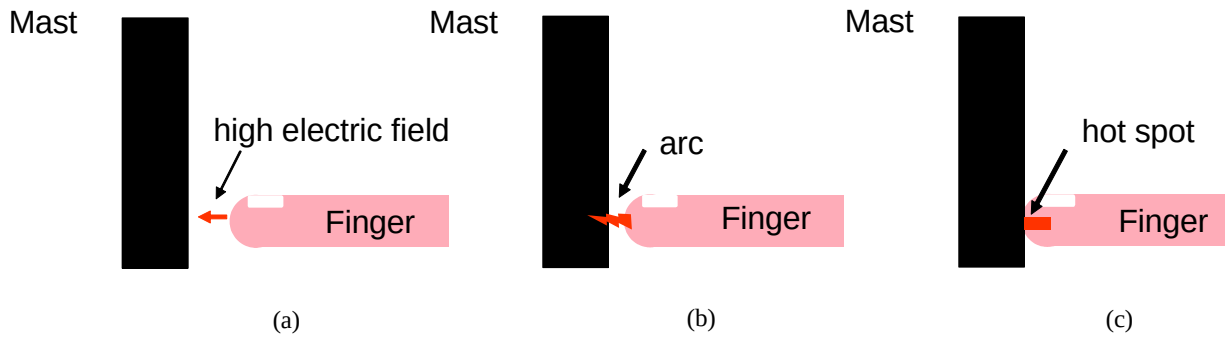

Figure 6-2
The steps in contact. (a) Before arc. (b) At point of arc. (c) At contact

7
MODELS FOR CALCULATING HIGH FREQUENCY CONTACT CURRENTS

In this section, several models will be introduced that will be used to calculate RF contact currents in the body that can lead to RF burns. The first two models relate to parasitically energized conductors (i.e., those that are energized by sources not attached to them). In the first case, the parasitic element is an ungrounded vertical mast while in the second, the parasitic element is an insulated fence grounded at the end opposite the contact. The last model is of a person in contact with a directly energized antenna.

Contact with an Ungrounded Mast Exposed to RF Electromagnetic Fields

To understand this phenomenon, a simple model was constructed. More specifically, the problem defined in Fig. 7-1a was set up and solved. In this problem a person is standing on perfect earth (i.e., $\sigma = \infty$) and is in contact with the bottom of a tall vertical cylindrical metallic mast (or cable) of height "h" and radius r_o. The mast/person combination is exposed to a vertically polarized, horizontally traveling plane wave of frequency "f" and amplitude E_o V/m.

As long as the directly induced currents in the body can be ignored, the system (all but the person) can be replaced by a Thevenin equivalent circuit as shown in Fig. 7-1b. The person, then can be represented as a simple two terminal impedance. In this case, the impedance will be assumed to be a resistor with a value of R_p = 1500 Ohms since "finger" contact is assumed [16]. Electromagnetic reciprocity theory used to analyze receiving antennas can also be used to analyze the system shown in Fig. 7-1a. For this, the terminals of the equivalent circuit shown in Fig. 7-1b are the points touched by the human's hand and foot shown in Fig. 7-1a.

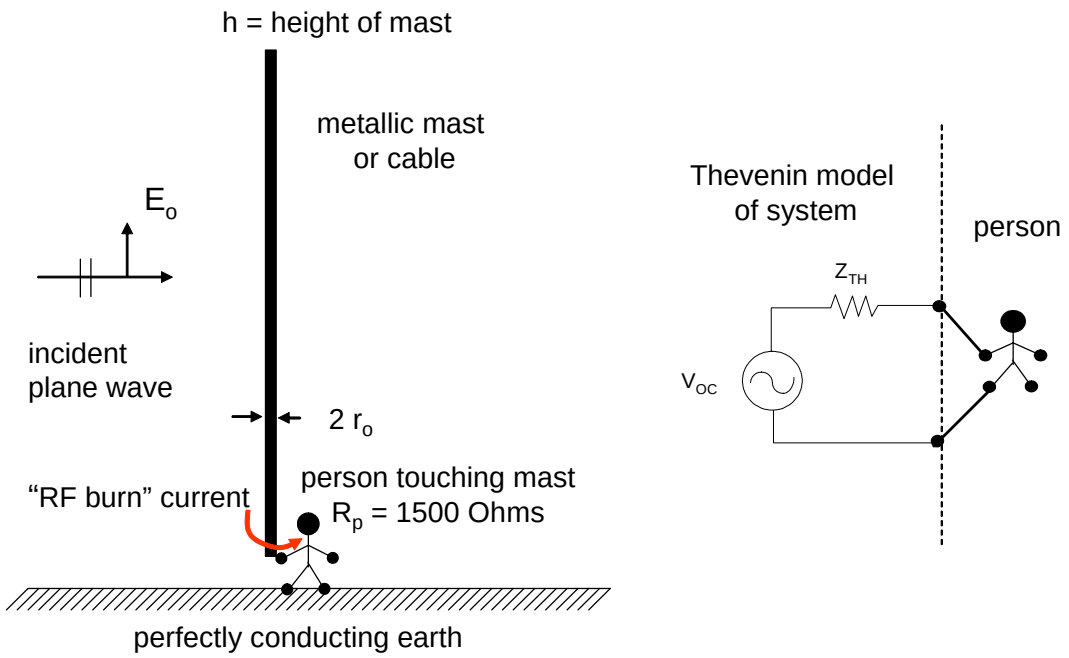

a) System (i.e., all except person) to be modeled

b) Thevenin Equivalent

Figure 7-1
Geometry of the ungrounded vertical mast problem and its equivalent circuit.

Simple analytic expressions for the open circuit voltage (V_{oc}) and Thevenin impedance (Z_{th}) in Fig. 7-1b have been developed in Appendix A. From these simple expressions, insight can be obtained into the behavior of the contact current in limiting cases and the effect of different problem parameters can be made more clear. For example, from Equations (A5) and (A11) of the appendix, it is shown that, at low frequencies, the open circuit voltage is roughly constant with frequency and the Thevenin impedance is capacitive and quite large compared to the body impedance (i.e., approximately 12.5 volts and 10 kΩ respectively at 100 kHz for a 25 meter high 12.5 cm radius mast in a 1 V/m incident electric field). Since the Thevenin impedance is capacitive and dominates the impedance of the person, the contact current is small (i.e., 1.5 mA at 100 kHz) and a linear function of frequency. However, as the frequency is increased beyond the quasi-static limit (i.e., βh is no longer small compared to 1), the Thevenin impedance becomes small (e.g., hundreds of ohms) compared to the body resistance so that the contact current is now limited by the body resistance while the Thevenin voltage increases only slightly (i.e, 16 volts at 3 MHz). At this frequency, the contact current is approximately 11 mA. As illustrated in Fig. 7-2, the peak current occurs at the first resonance of the mast when its electrical height is approximately λ/2 where λ (the wavelength) = 300/f(MHz) meters. Unfortunately, the simple formulas in (A5) and (A7) – (A9) cannot be used to calculate this peak current due to an artifactual "notch" and the numerical results introduced below will have to suffice[2].

[2] The "notch" in the analytical result is an artifact of the specific method used that occurs because the current on the wire is assumed to have exactly sinusoidal variation along the wire's length and the input impedance is normalized to this current. At certain frequencies the wire current is then exactly zero and the impedance predicted to be infinite. This is what leads to the artifact.

A plot of the current injected into a person with a body resistance of 1500 Ohms and in contact with a 25 meter high 12.5 cm radius mast in a 1 V/m incident electric field is shown in Fig. 7-2. In addition to the "analytic" result from which the behavior discussed above can be observed, there are two other results based on numerical solutions to electromagnetic problems. The first numerical result is a computation using the finite difference time domain (FDTD) method mentioned earlier. In this method the 1500 Ohm body resistance was constructed with a physical model that will be examined more carefully later in the report in the context of studying the effects of direct interaction with the body at higher frequencies. More details of the FDTD method will be given later. The second is labeled "MoM" and is based on an independent numerical method called the method of moments (MoM) [17]. The three results are in reasonable agreement except for the anomalous notches in the analytic result that are discussed in the earlier note. The numerical results are included for several reasons. First, they can be used to calculate the contact current near resonance when the simple analytical result fails. Second, they validate the simple approximate analytical result. Third, the general agreement between all results provides confidence that numerical results are valid. Finally, numerical methods (especially the FDTD) can be used at higher frequencies than the analytical method since the simple body impedance model is no longer valid.

Of perhaps most interest here is that the largest contact current occurs at the first resonance of the mast which is when the height of the mast is approximately one half wavelength. At higher order resonances, only a smaller portion of the mast effectively gathers energy due to destructive interference effects between currents gathered from different portions of the mast. This results in an effectively shorter mast.

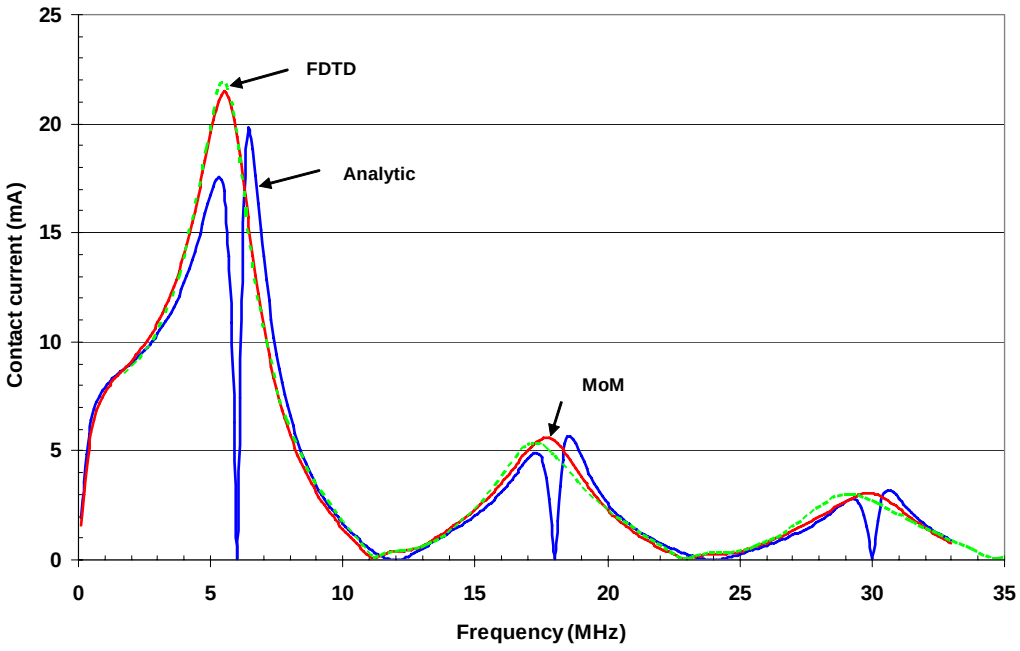

Figure 7-2
Contact current injected into a person with R_p = 1500 Ω (E_o = 1 V/m, h = 25 m, r_o= 12.5 cm).

While it is important to note that the peak contact current occurs when the vertical conductor is approximately equal to one-half wavelength in height (i.e., the first resonance), the contact currents for lower frequencies than the first resonance must not be neglected. Consider, for example, the AM radio broadcast band (0.535 to 1.710 MHz), where the wavelengths are relatively long (i.e., 176 m to 560 m) or half-wavelengths ranging from 88 m to 280 m and most antennas radiate vertically polarized fields. For most practical situations near such an antenna, the taller the conductor, the more severe the open circuit voltage and available contact current. Figure 7-3 illustrates this effect for a frequency of 1 MHz and a range of vertical conductor heights up to 914 m or about three wavelengths. It is apparent that the critical parameters related to the potential for RF burns increase rapidly with increasing height of the conductor up to 150 m, a significant height. This means that the hazard of RF burns increases for taller structures when in the environment of AM broadcast stations. For example, exposure to tall cranes is worse than exposure to shorter cranes.

Why There Is a Diminishing Probability of RF Burns at Higher Frequencies

From the Appendix A Equation A10 for the quasi-static open circuit voltage at the mast terminals, it appears that the taller the mast, the larger the open circuit voltage. But, there is a limit to this increase because at some point the height of the mast is no longer a small fraction of a wavelength and the open circuit voltage no longer increases linearly with mast height. As mentioned above, the voltage reaches its maximum when the mast is a half wavelength in height.

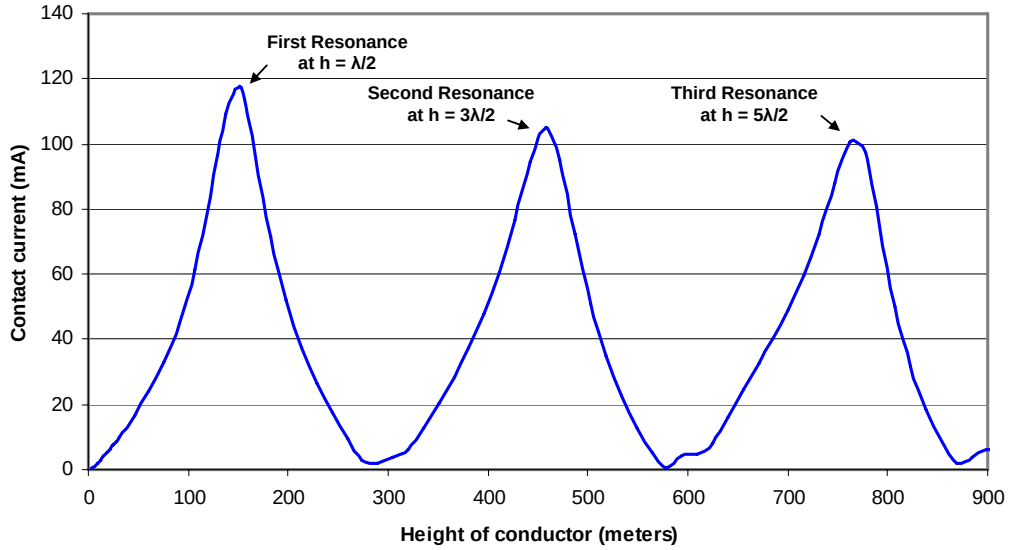

Figure 7-3
Contact current at base of a vertical conductor (radius is 1.25 cm) of varying height exposed to an electric field strength of 1 V/m at 1 MHz. Contact resistance is 1500 ohms. A half-wavelength of a 1 MHz signal is 150 m.

Figure 7-3 illustrates the oscillatory nature of the contact current with peaks in the current at odd integer multiples of a half-wavelength. It is relevant to note that while the contact current does go through peaks at greater heights, the maximum current is always greatest at the first half-wavelength and has decreasing peak values at greater heights. The most significant insight from

this type of analysis is that very long, or tall, conductors exposed to higher frequency fields, such as VHF transmissions, do not present the same maximum contact current values. This is dramatically illustrated in Fig. 7-4 where the contact current is plotted vs. conductor height for 1, 10, and 100 MHz. These data show why long conductors exposed to VHF RF fields do not present the same degree of potential for an RF burn as similar length conductors at lower (medium wave) frequencies.

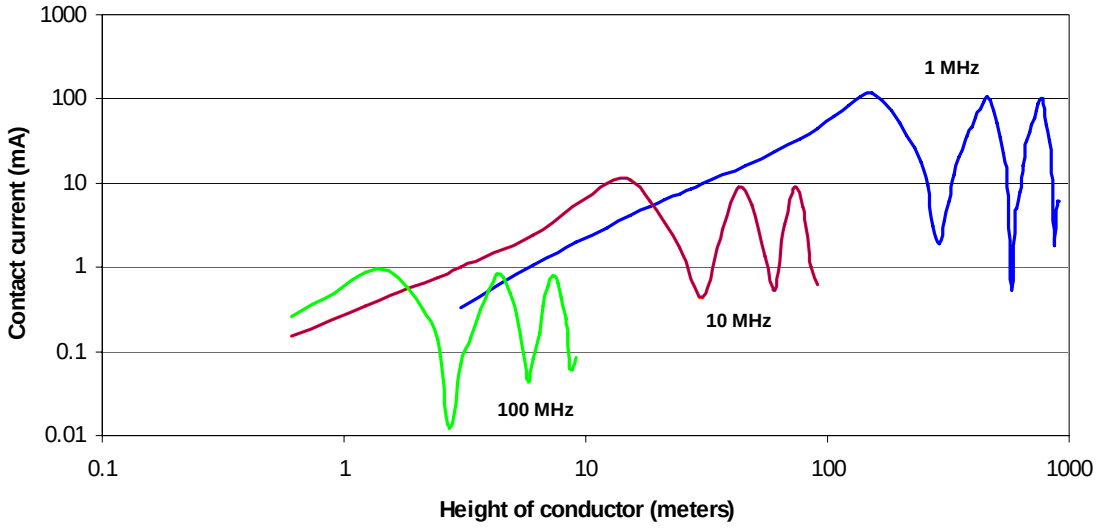

Figure 7-4
Calculated contact current vs. height of conductor exposed to an electric field strength of 1 V/m for frequencies of 1, 10, and 100 MHz. Note the similar behavior of the oscillation in contact currents but, importantly, the diminished value of the peak currents at higher frequencies.

A Simple Expression for the Maximum contact Current

Given the facts that the maximum contact current in Fig. 7-2 for a 1500 Ω person is approximately 20 mA at 6 MHz, that parametric studies show that the contact current is proportional to the half wavelength resonant length of the mast (i.e, inversely proportional to the first resonance frequency) and that the contact current is proportional to the incident electric field strength, the maximum possible contact current due to contact with a vertical mast can be written as

$$I_{contact}\ (max) = (120\ E_o)/f(MHz)\ mA \qquad \textbf{Eq. 7-1}$$

where E_o is in volts per meter and f is the frequency in megahertz. Since the person's 1500 Ω resistance dominates the input impedance of the antenna, the maximum open circuit voltage is approximately

$$V_{oc}(max) = (180\ E_o)/f(MHz)\ \ volts \qquad \textbf{Eq. 7-2}$$

This result is very interesting since it can be inferred that the open circuit voltage can be substantial even in a relatively weak incident electric field (i.e., in the 6 MHz case, the voltage is the electric field multiplied by 30). Very roughly, the maximum open circuit voltage at any given frequency is the electric field multiplied by a numerical value equal to one half wavelength in meters at that frequency. Of further interest is the fact that at 6 MHz, the incident electric field required to exceed the Navy and IEEE open circuit voltage of 140 volts to protect against RF burns is approximately 4.7 volts per meter, much smaller than the FCC MPE limit for direct exposure to electric fields at this frequency (i.e., 614 V/m). In addition, the contact current for this situation is approximately 100 mA, a result that will be shown later to be large enough to cause an RF burn.

This approximation to the "maximum" contact current is fairly consistent with what is shown in Fig. 7-2. As the frequency goes up the maximum contact current available at higher order resonances is decreased because the electric field is "collected" from a smaller length of mast because the contributions from different parts of the mast destructively interfere with each other due to phase shifts as they travel along the mast.

Given Eq. 7-1 and the fact that the contact current at higher order resonances is smaller than Eq. 7-1, it is clear that as the frequency is increased the largest possible contact current (i.e., that which occurs when a human touches a half wavelength mast) is reduced. It follows that the electric field exposure required to cause an RF burn at the point of contact is increased as well. At some frequency the FCC MPE limit is large enough that it may be protective against RF burns as well as against exposure of isolated bodies. Hence, at higher frequencies than this, it may not be necessary to limit contact current from passively excited wires separately.

If the human impedance is assumed to be 1500 Ω and 100 mA is taken as the threshold for an RF Burn, then the electric field at which RF burns may occur is

$$E_o(\text{threshold for RF Burns}) = 0.83\ f(\text{MHz})\ \text{V/m} \qquad \textbf{Eq. 7-3}$$

The FCC MPE limits (occupational) for electric field exposure are

614 V/m	0.3 – 3.0 MHz
1842/f(MHz) V/m	3.0 – 30 MHz
61.4 V/m	30 – 300 MHz

Given these limits, the frequency above which the MPE limit would become protective of RF burns (from touching ungrounded vertical masts that are parasitic antennas), with the assumption that the only criteria for a burn is a contact current of 100 mA, is approximately 75 MHz. This does not cover the case for touching directly energized antennas or address the issue of potential RF burn hazard from electrical arcs that may carry less than 100 mA of current. These matters will be studied during a future segment of this project.

Contact with a Fence Exposed to RF Electromagnetic Fields

Consider next the geometry shown in Fig. 7-5. Here a person is in contact with a long fence with its area in the plane of a vertically polarized incident plane wave (the plane wave's magnetic field is perpendicular to the area of the fence). Again, it will be assumed that the earth is perfectly conducting (this condition can be relaxed if needed) and that the fence is "grounded" at one end.

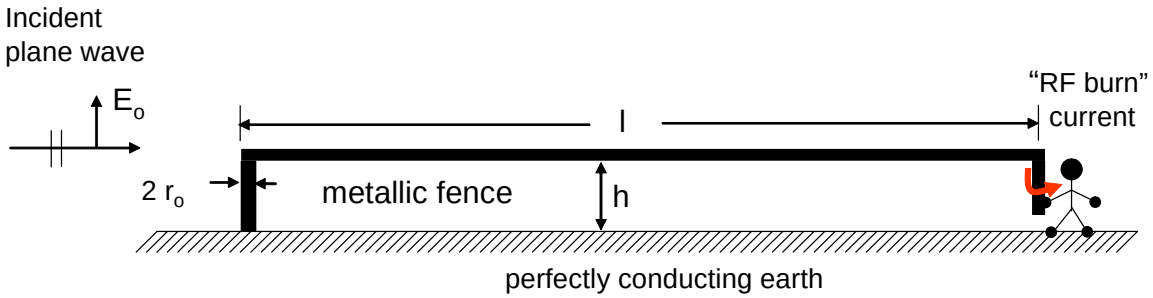

Figure 7-5
Geometry of the grounded fence problem. As shown in the figure, the incident wave comes from the left and is vertically polarized (i.e., the electric field is vertical).

Again, the approach will be to identify a Thevenin equivalent circuit for this "system" identical to that shown in Fig. 7-1b. The details of this calculation are given in Appendix B.

The results of a calculation of RF current injected in a person with $R_p = 1500\ \Omega$ are plotted in Fig. 7-6. At 1 MHz, quasi-static theory from Appendix B can be used. For the conditions of Fig. 7-6, $V_{oc} \approx 1.7$ volts and hence (since $Z_{th} << 1500\ \Omega$) the contact current is approximately 1.1 mA in rough agreement with the value shown in Fig. 7-6. The largest contact current occurs when the length of the fence at its first resonance (i.e., approximately one fourth of a wavelength or when the total length of the equivalent loop is one half wavelength). This result would seem to indicate that maximum contact current would decrease with the length of the fence. However, since by Faraday's law, the voltage induced in a loop is proportional to the time derivative of the magnetic field (i.e, proportional to the frequency for sinusoidal currents) the two effects offset and the maximum contact current is roughly independent of frequency. Given this result and the fact that the Thevenin impedance is much larger than the impedance of a person at this resonance frequency, the maximum contact current can be estimated very simply as

$$I_{contact}\ (max) = 4E_o h\ mA \qquad \textbf{Eq. 7-4}$$

Where E_o is in V/m and h is in meters. It is expected that this result should hold as long as the height of the fence is electrically small. Note that by comparing Eqs. 7-1 and 7-4, it is evident that in most cases, the probability of an RF burn from a fence is smaller than that from a vertical mast. For this reason, it will be assumed here that the vertical mast case is the "worst case."

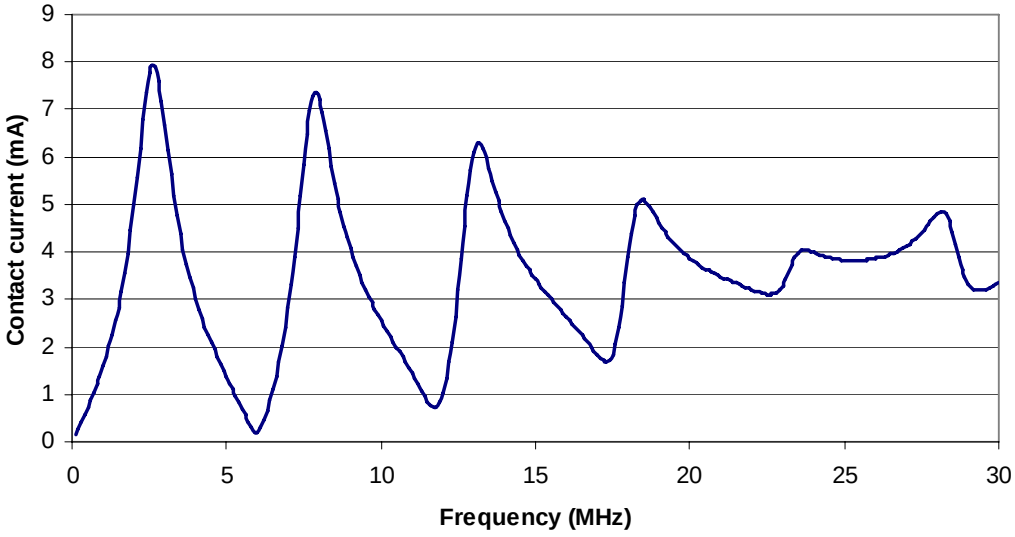

Figure 7-6
Current induced in a person touching a fence with R_p = 1500 Ω (E_o = 1 V/m, h = 2m, r_o= 0.1 cm, l = 25 m).

As in the case for a vertical mast, RF burns can occur at electric field exposures less than the FCC MPE limits. More specifically, if the RF burn threshold is 100 mA, and the fence height is 1 meter, then RF burns could potentially occur if the incident electric field is 25 V/m, a value significantly less than the MPE limit up to 30 MHz. Beyond this frequency, the simple model is not expected to be accurate since the fence height may no longer be electrically small.

Discussion of Why There are Diminishing RF Burns at Higher Frequencies

According to Fig. 7-6, the peak contact current is reduced at higher order resonances since open circuit voltage will also decrease due to destructive interference from induced voltages on different parts of the fence. Hence, (5) represents a rough maximum on the contact current that is available from a fence exposed to RF electromagnetic fields.

Contact with a Directly Energized Antenna

Consider the situation shown in Fig. 7-7. Here the person is in contact with a directly energized antenna rather than a parasitically excited mast. For this case the potential for an RF burn may be larger than for the parasitically excited case.

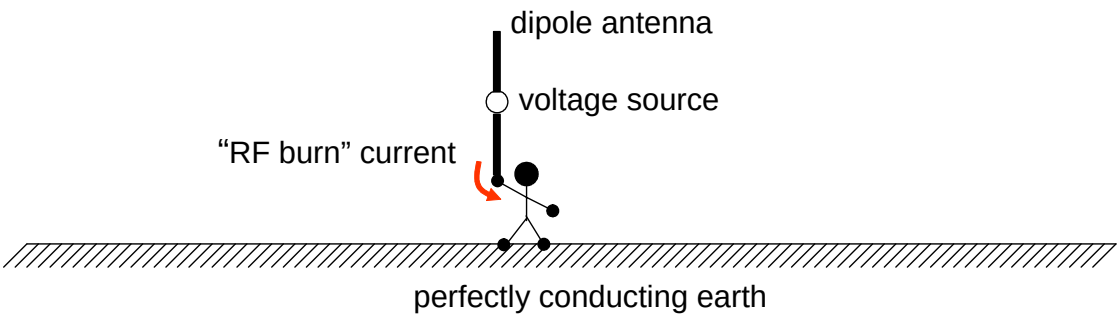

Figure 7-7
Person in direct contact with a dipole antenna.

In the second phase of this research project, a model will be developed to calculate the contact currents for this case.

Model for Predicting the Minimum Contact Current Needed to Cause an RF Burn

In Fig. 7-8, the details of the contact between a mast (or cable) and a finger are shown. It is assumed that there is a steady state current traveling from the tower (or mast) to the finger and that this current is the one that has been calculated using the previously developed models. The purpose of this section is to approximate the current density in the finger and the associated temperature rise that could lead to a burn.

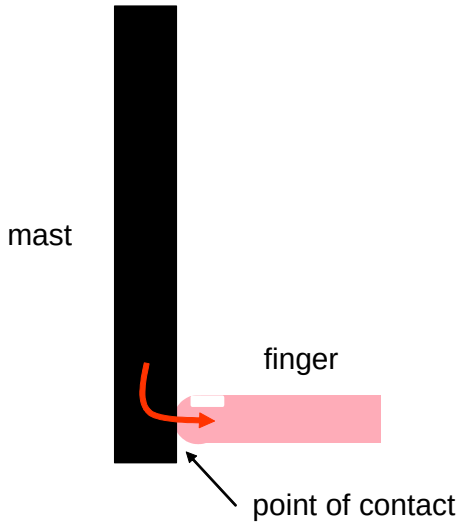

Figure 7-8
Contact between a finger and an energized mast.

It is assumed that the contact area between mast and finger is circular as illustrated in Fig. 7-9 and that the diameter of this contact area is "r." Then, the current density in the finger at the point of contact is

$$J = \frac{I}{\pi r^2} \quad A/m^2 \qquad \textbf{Eq. 7-5}$$

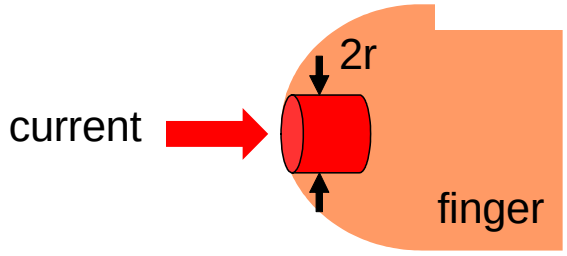

Figure 7-9
Simplified model for current flow and temperature rise in the finger.

The power absorbed per unit volume is then

$$P_a = \frac{J^2}{\sigma} \quad W/m^3 \qquad \textbf{Eq. 7-6}$$

where σ is the conductivity of the tissue (assumed here to be σ = 0.6 S/m) [18].

The local SAR (power absorbed per unit mass) is given in Eq. 1-1 as

$$SAR = \frac{J^2}{\sigma d} = \frac{\sigma E^2}{d} \quad W/kg \qquad \textbf{Eq. 7-7}$$

where "d" is the density of flesh (assumed to be 1000 kg/m^3) [18].

If it assumed that the radius of the contact point is 0.25 cm and the current into the contact point is 10 mA, then the local SAR is 432 W/kg, more than 43 times the local basic restriction for controlled environments used in the IEEE standard of 10 W/kg averaged over 10 g of tissue [3]. If the radius of the contact point is half of this value (i.e., 0.125 cm), then the local SAR is 1,730 W/kg. This radius is equivalent to that for the RF burn shown in Fig. 7-10.

Figure 7-10
Typical RF burn on finger.

The final step in determining whether a burn can occur is to assume adiabatic heating and to then calculate the temperature rise at the contact point as a function of time.

This temperature rise can be written as

$$dT = \frac{SAR}{c} \ ^{o}C/second \qquad \textbf{Eq. 7-8}$$

where SAR is in watts/kg and c (the specific heat) is approximately 3500 joules/(kg - ^{o}C) assuming that the body is mostly water [18]. For the example given above (i.e., SAR = 1730 W/kg) dT = 0.49 ^{o}C/sec, probably too small to cause a burn. The reason is that the temperature needed to cause a burn in a short time is approximately 55 ^{o}C [12]. During the 37 seconds required to "heat" the tissue from 37 ^{o}C (approximate body temperature) to 55 ^{o}C, cooling mechanisms would generally be activated.

If, however, the RF burn current is 100 mA, the temperature rise would be 49 ^{o}C/sec and it would take only 0.37 second to raise the temperature from body temperature (assumed to be about 37 ^{o}C) to 55 ^{o}C. A graphical presentation of these data is shown in Fig. 7-11.

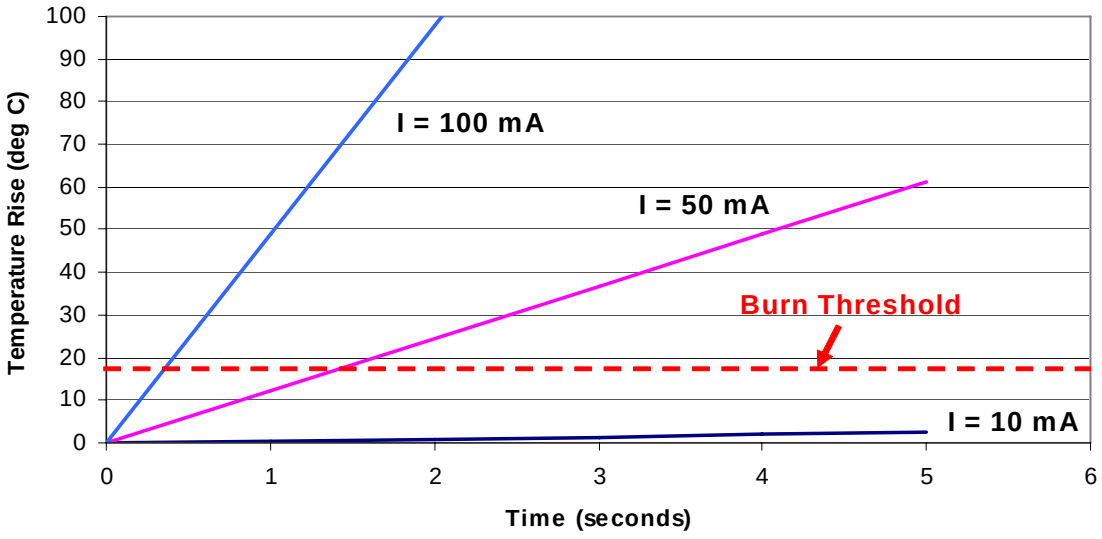

Figure 7-11
Local adiabatic temperature rise in a finger due to RF current.

What Are the Limitations of the Mast and Fence Models Introduced Above?

It was explicitly stated that the model discussed above is valid only when the direct interaction with the body can be neglected. While this is likely to be true when the body is a "small fraction of a wavelength" in maximum dimension, it is important to know this more precisely. For this purpose, it was decided to study this problem using a full wave numerical technique (FDTD) and comparing those results with the method described here.

FDTD Modeling of Contact Current

Some of the technical details concerning the FDTD method are described briefly in Appendix D. As discussed there, the method discretizes the space over which the electromagnetic fields are of interest. Each discrete location (or cell) in space can have its material properties set to whatever value is appropriate. Provided the space is discretized sufficiently finely (so that there are approximately 10 samples per wavelength at the highest frequency of interest), the method can accommodate any distribution of material without increasing the computational complexity or the time required to perform a simulation. Thus, the operations performed by the FDTD method are essentially the same whether a volume is devoid of material (i.e., filled with free space) or the volume is filled with a complicated, inhomogeneous arrangement of various materials.

Here no attempt will be made to exploit the full computational power or flexibility of the FDTD method. Rather, a simple model will be used and then some geometric variations will be introduced to show how those variations affect the flow of current. All the simulations use the same underlying "computational engine." The only things that change from one simulation to the next are the coefficients used to describe the material properties at locations throughout the FDTD grid.

The results shown in Fig 7-2 were based on a "human" who was treated as an electrically small lumped element of 1500 ohms. (The word human will be used here as being synonymous with the resistor model that exists at the base of the mast.) With the exception of the notch in the analytic results, the results produced by the FDTD method, the method of moments (MoM), and the analytic approach agreed well.

In the case of the FDTD method, the human was modeled as a single "cell" in the grid. The spacing between cells for this particular simulation was $\delta = 0.25$ m. The geometry is depicted in Fig. 7-12(a) (this figure is not drawn to scale—the height of the mast is 25 m, which is 100 times greater than the height of the lumped-element human). The material parameters for the cell at the base of the mast were chosen to realize a dc resistance of 1500 ohms across this cell. For this simulation there is no distinction between the current flowing at the point of contact with the mast or the point of contact with ground plane—the current is the same throughout the cell.

As a first refinement, the model of the human can be allowed to be more realistic in terms of height. Figure 7-12(b) depicts the geometry when the human consists of three cells. (For all the results to follow, the top of the mast remains at 25 m, (i.e., h is fixed). Hence, as the human gets taller, filling more of the space beneath the mast, the length of the mast decreases but the height stays unchanged. Additional simulations were done where the length of the mast was fixed at 25 m. Thus, as the height of the human increased, the highest point of the mast correspondingly increased. The difference in the currents between maintaining a constant height or maintaining a constant length were small.) The material parameters of each cell are chosen so that the total dc resistance from the top of the human to the bottom remains 1500 ohms. Now the difference between the current at the point of contact with the mast and any other location in the expanded model of the human can be investigated.

Figure 7-13 shows the current that flows in two different models of the human. (In this plot and the following three, the configuration that produces the highest average current will be plotted with a red solid line.) The "short" model is a single 1500 ohm resistor with a height H of 0.25 m and is the same as used to generate the results shown in Fig. 7-2. The "tall" model consists of eight segments such that the height H is 2.00 m. The total resistance across all the segments remains 1500 ohms. However, since resistance is proportional to length, and the length of the tall model is eight times greater than the length of the short model, the conductivity associated with each individual cell in the tall model is eight times greater than the conductivity used in the short model. The plot shows the current in the highest segment (the one that contacts the mast) and the lowest segment (the one in contact with the ground plane). Note that although the current at the base of the tall model is less than that of the short model, the current in the segment in contact with the mast is larger than that obtained from the single lumped element of the short model.

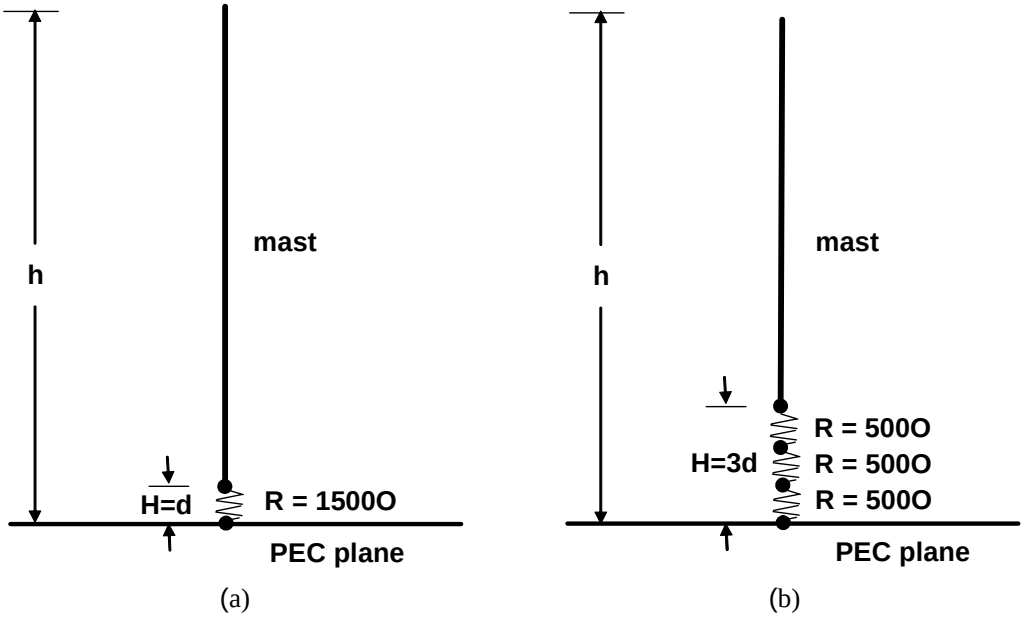

Figure 7-12
(a) Lumped-element model of a human in contact with the base of the mast. (b) Model that uses multiple cells in the FDTD grid to model the human. This sketch shows three cells (subsequent results will use eight cells). The conductivity of the cells in the "tall" model are such that the resistance across the entire human is maintained at 1500 ohms.

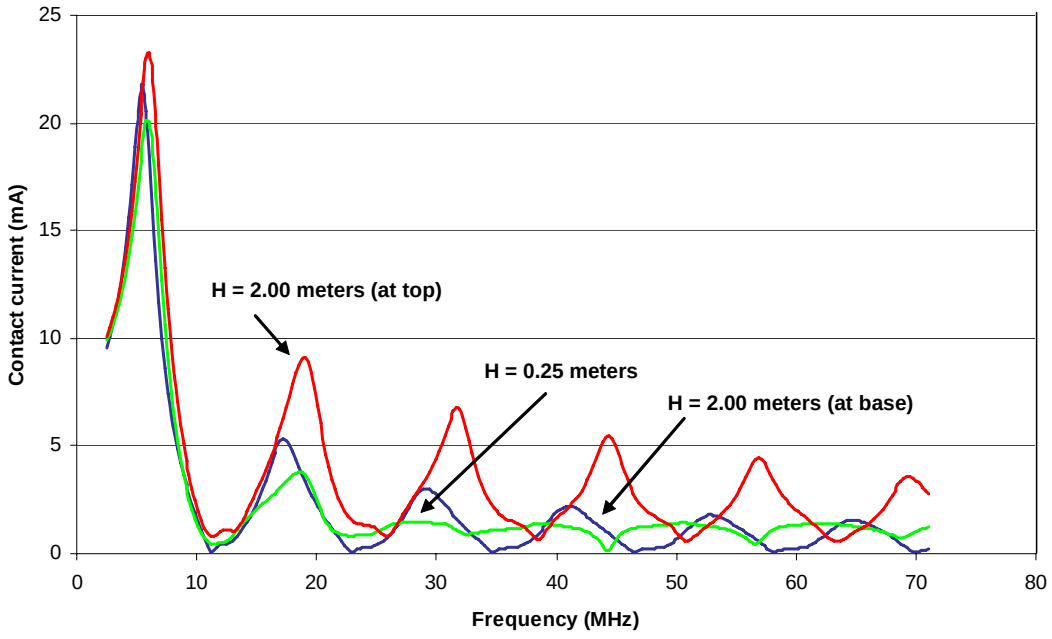

Figure 7-13
Currents in different models of the human. The "short" (H = 0.25 m) model corresponds to a single cell in the FDTD grid being used to approximate the human. The "tall" results (H = 2.00 m) use eight cells in order to realize a model that is 2.00 m high. The current at both the cell in contact with the mast (labeled "at top") and the one in contact with the ground plane (labeled "at base") are shown. h = 25 m, R = 1500 ohms.

It should be noted that the method of moments can also be readily used to investigate the currents that flow in the tall model. The tall model is still effectively a "wire frame" model in which conduction currents flow in linear segments. (MoM results for the tall model were compared to the FDTD results shown in Fig. 7-13 and the agreement was excellent.) However, with the introduction of displacement currents, which will be considered next, or a "wide" model of the human where currents are not restricted to flow in only one direction, the method of moments becomes much more cumbersome. On the other hand, the FDTD implementation is essentially unchanged by the introduction of these features.

In the FDTD method one can set the conductivity *and* the permittivity for each cell (permeability can also be set for each individual cell, but we assume non-magnetic materials and hence leave the permeability as that of free-space). The previous results varied only the conductivity for a cell and left the permittivity to be that of free space. In practice a human has permittivity that can be quite different from that of free space. The permittivity is a function of the tissue (e.g., muscle, fat, bone, etc.) and the frequency. As a simple refinement to the model, let us merely consider the case where the relative permittivity ε_r is either 1.00 (free space), 4.00, or 8.00. Figure 7-14 shows the currents that flow in the short model, i.e., H = 0.25 m. Note that the current increases significantly as the permittivity increases and the amount of increase is more pronounced at higher frequencies (as one approaches dc, the different permittivities should not and do not affect the current).

As depicted in Fig. 7-15, another simple improvement to the model is to allow the human to be wider than it is deep (i.e., wider across the shoulders than through the chest). Since the FDTD method allows one to set the material parameters of cells to whatever is desired, let us consider the case of a rectangular human who is 2.00 m tall, 0.75 m wide, and 0.25 m deep. The material parameters are such that the total resistance from top to bottom is still 1500 ohms. Resistance is inversely proportional to cross-sectional area. Thus, because the wide model has three times the cross-sectional area as the thin one, the conductivity associated with any cell in the wide model is three times less than in the thin model. Figure 7-15 shows the current in the cell in contact with the mast for both the wide and the thin model. In this case the permittivity is again that of free space. The contact current for the thick model is seen to be less than for the thin model (as would be expected from the decreased conductivity).

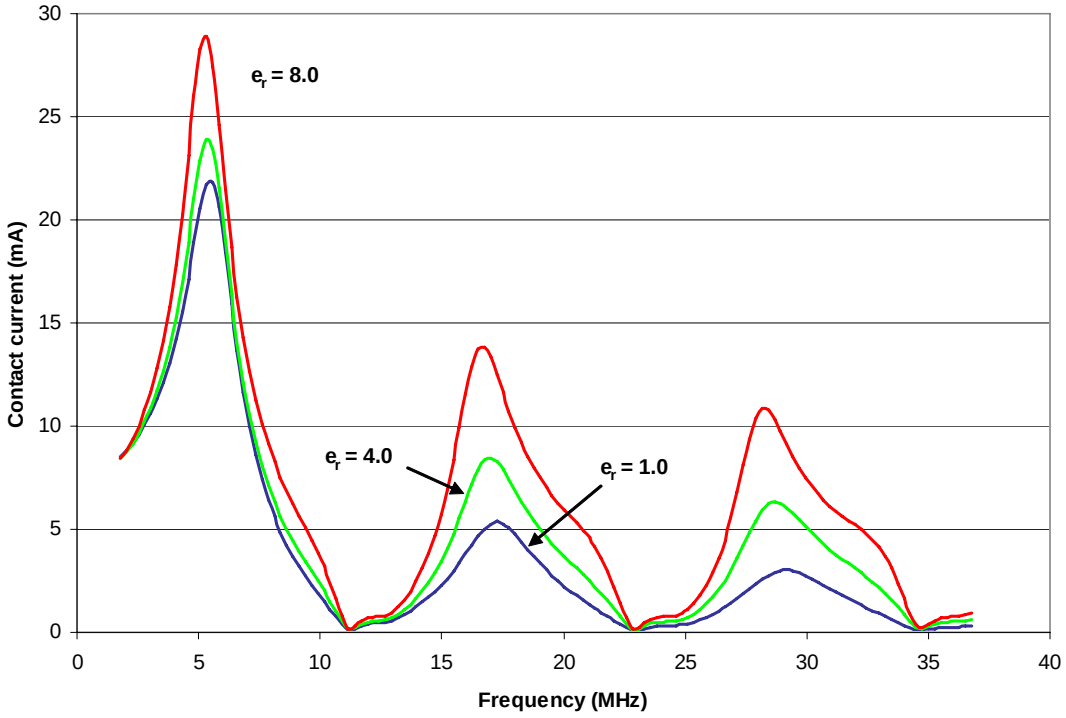

Figure 7-14
Current in the 1500 ohm resistor when the relative permittivity of the cell is either 1.00, 4,00 or 8,00. Here the short model is used, i.e., H = 0.25 m. h = 25 m

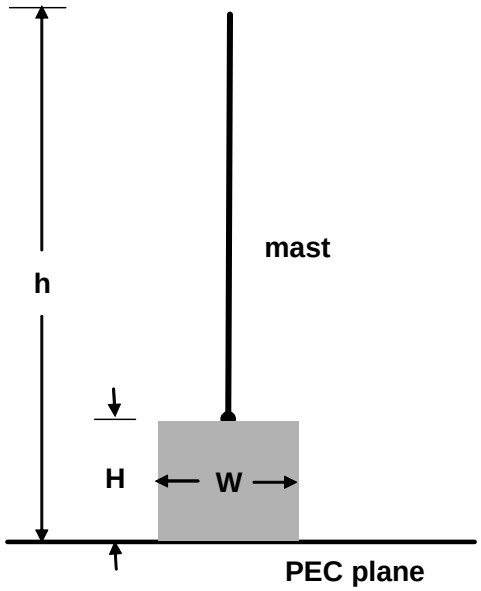

Figure 7-15
Sketch of a "wide" model of the human. In the results to follow, the human will be eight cells high, three cells wide, and one cell thick. The mast makes contact with the center of the human. The cell directly below the mast is the one in which the current is measured.

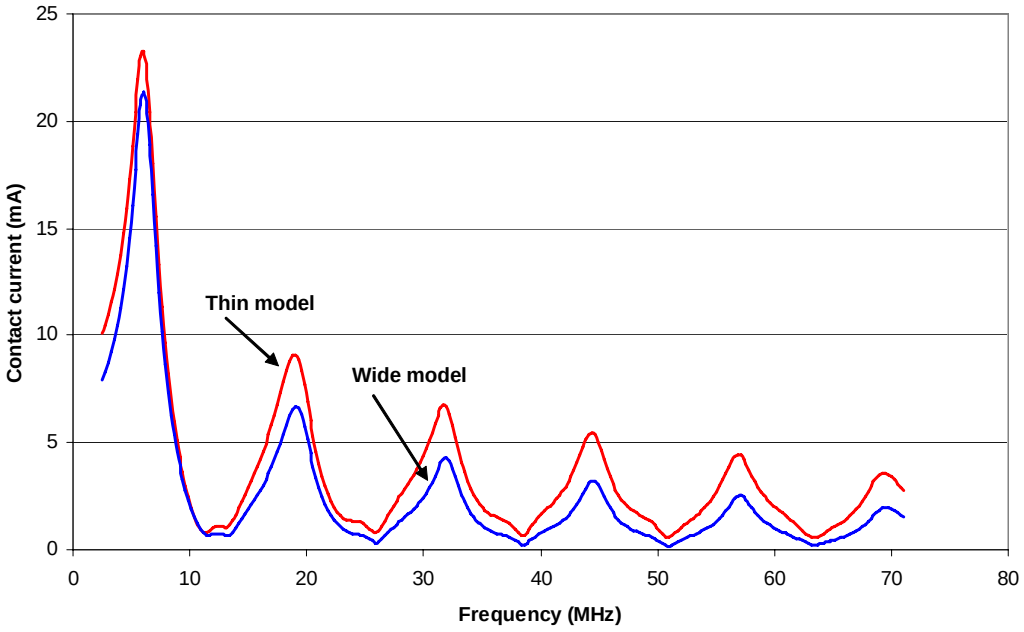

Figure 7-16
Current in the cell in contact with the mast when the human is 2.00 m high. The "thin" results correspond to a model of a single line of resistors directly below the mast (the cross-sectional dimensions are 0.25 m by 0.25 m). The "wide" results corresponds to a model that has cross-sectional dimensions of 0.75 m by 0.25 m. h = 25 m, R = 1500 ohms.

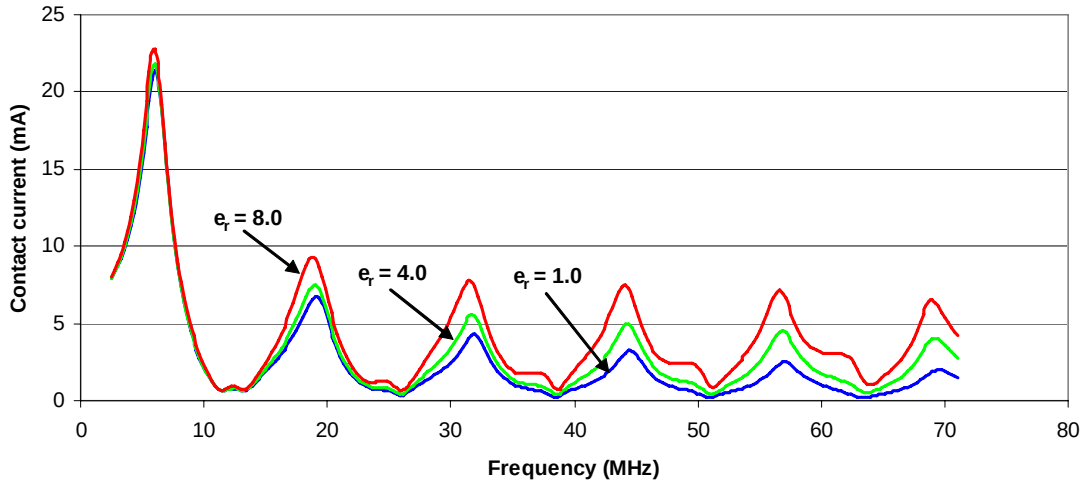

Figure 7-17
Current in the cell in contact with the mast for the wide model. The relative permittivity is either 1.00, 4.00 or 8.00.

The results presented here were produced using very simple physical models. They are intended merely to illustrate that the current can change significantly with changes to the underlying geometry even when the lumped (dc) properties are not changed. The FDTD method provides quite a bit of additional freedom in modeling than is explored here. For example, there is no reason the human has to be placed beneath the mast (that was done to provide easy comparison with the analytic method and the method moments). The human could be beside the mast and contact could be through an outstretched arm or finger. By using a finer discretization one could add a great deal of geometric fidelity to the human. One could also incorporate different material constants to account for different tissue throughout the body.

Conclusions

Analytical and numerical electromagnetic models for two important cases that are useful for predicting RF burns at higher frequencies than previously possible have been developed. The specific cases considered are for humans touching vertical masts and horizontal fences that are exposed to electromagnetic fields from nearby sources. Each model is augmented by a theory that relates the contact current with temperature rise near the point of contact. The models can be used to determine the threshold conditions for which an RF burn could occur. In addition, a strategy for extending these models to even higher frequencies has been developed. The higher frequency models will utilize the Finite Difference Time Domain (FDTD) method and incorporate an anatomically correct model for a human.

The models developed in this study indicate that:

- If the human impedance is assumed to be 1500 Ω and 100 mA is taken as the threshold for an RF Burn, then the threshold electric field at which an RF burn occurs from contact with a vertical mast at its first resonance (i.e., the worst case that occurs at 150/f(MHz) meters) is approximately E_o = 0.83 f(MHz) V/m,
- The electric field required to cause an RF burn is larger than 0.83 f(MHz) V/m if the frequency is above or below the first resonance of the vertical mast,
- At frequencies below the first resonance, the probability of an RF burn is greater for contact with tall metallic objects than for short metallic objects,
- For a given electric field exposure level, the probability of an RF burn decreases with frequency at a rate of approximately 1/f(MHz),
- At frequencies below approximately 75 MHz, RF burns can occur at electromagnetic field levels less than the maximum permissible exposure in the most widely used RF Safety standards
- At frequencies higher than the first resonance, contact with taller metallic objects does not result in a greater probability of RF burns than contact with shorter metallic objects.

8
REFERENCES

1. EPRI, EPRI AC Transmission Line Reference Book – 200 kV and Above, Third Edition, Chapter 7, EPRI, Palo Alto, CA, 2005

2. Bailey, W.H. and J. A. Nyenhuis, "Thresholds for 60-Hz Magnetic Field Stimulation of Peripheral Nerves in Human Subjects," Bioelectromagnetics, Vol. 26, pp. 462–468, 2005.

3. IEEE, "IEEE Standard for Safety Levels with Respect to Human Exposure to Electromagnetic Fields, 0–3 kHz," IEEE Standard C95.6 – 2002, IEEE, 3 Park Avenue, New York, NY, 10016-5997.

4. http://www.fcc.gov/oet/rfsafety/

5. Rogers, S.J. "Radiofrequency Burn Hazards in the MF/HF Band." In J.C. Mitchell (ed.)., USAFSAM Aeromedical Review 3-81, Proceedings of a Workshop on the Protection of Personnel against RFEM, pp. 76-89, 1981.

6. Gandhi, O.P., I. Chatterjee. "Radio-Frequency Hazards in the VLF to MF Band." Proc. IEEE, Vol. 70, No. 12, pp. 1462-1464, 1982.

7. Reilly, J. P., Applied Bioelectricity, Springer, New York, 1998.

8. Chatterjee, I., D. Wu, and O.P. Gandhi. "Human Body Impedance and Threshold Currents for Perception and Pain for Contact Hazard Analysis in the VLF-MF Band." IEEE Trans. Biomed. Eng., Vol.33, No. 5, pp. 486-494, 1986.

9. W. H. Hayt, Jr. and J. A. Buck, Engineering Electromagnetics, pp. 369-376, 2001.

10. http://www.osha.gov/SLTC/radiofrequencyradiation/healtheffects.html

11. http://safetycenter.navy.mil/acquisition/RFR/rfr.htm#RF_Burn

12. IEEE, "IEEE Standard for Safety Levels with Respect to Human Exposure to Radio Frequency Electromagnetic Fields 3 kHz to 300 GHz," IEEE Standard C95.1 – 2005, IEEE, 3 Park Avenue, New York, NY, 10016-5997

13. International Commission on Non-Ionizing Radiation Protection (ICNIRP), "Guidelines for Limiting Exposure to Time-Varying Electric, Magnetic, and Electromagnetic fields (up to 300 GHz)," ICNIRP Secretariat, c/o Dipl-Ing. Rtidiger Matthes, Bundesamt fur Strahlenschutz, Institut fur Strahlenhygiene, Ingolstadter Landstrasse 1, D-85764 Oberschleissheim, Germany.

14. B. Hocking and R. Westerman, Radiofrequency Electrocution (196 MHz), Occupational Medicine, *Vol.* 49, No. 7, pp. 459-461, 1999.

15. http://safetycenter.navy.mil/acquisition/RFR/rfr.htm#RF_arcs

16. Y. Kamimura, K. Komori, M. Shoji, Y. Yamada, S. Watanabe and Y. Yamanaka, "Human Body Impedance for Contact Current Measurements in Japan," Institute of Electronics, Information and Communication Engineers, Vol. E88-B, No. 8, August 2005, pp. 3263 – 3267.

17. R. F. Harrington, Field Computation by Moment Methods, Wiley – IEEE Press, New York, 1993

18. http://www.emfdosimetry.org/handbook4/handbook4.pdf

A
ANALYTIC THEVENIN IMPEDANCE MODEL FOR THE VERTICAL MAST

The purpose of this derivation is to illustrate how an analytic closed form model for the Thevenin equivalent circuit of a vertical mast over a perfect ground illuminated by a vertically polarized plane wave can be derived. This model is useful because it is relatively simple and can be used quickly to evaluate the effect of various parameters.

Using electromagnetic reciprocity theory, (assuming a z oriented wire), the open circuit voltage of the source shown in Fig. 7-1 is

$$V_{oc} = \frac{1}{I_{in}} \int_0^h E_{inc} \bullet I_t(z)\, dz \quad V \qquad \textbf{Eq. A-1}$$

where E_{inc} is the incident electric field, $I_t(z)$ is the current on the structure when excited by a voltage source at its terminals and I_{in} is $I_t(0)$, the current at the terminals [A1]. A reasonable approximation for $I_t(z)$ is

$$\begin{aligned} I_t(z) &= I_m \sin[\beta(h-z)] \quad A \\ I_{in} &= I_t(0) = I_m \sin(\beta h) \quad A \\ \beta &= \omega\sqrt{\mu_o \varepsilon_0} \quad rad/m \end{aligned} \qquad \textbf{Eq. A-2}$$

Let E_{inc} be a vertically polarized plane wave incident from the left

$$E_{inc}(x) = E_o e^{-j\beta x} \bar{a}_z \qquad V/m \qquad \textbf{Eq. A-3}$$

where a_z is a unit vector in the z direction

Then,

$$V_{oc} = \frac{1}{\sin(\beta h)} \int_0^h E_o \sin[\beta(h-z)]dz = \frac{E_o}{\beta \sin(\beta h)}(1-\cos(\beta h)) \quad V \qquad \textbf{Eq. A-4}$$

The equation can be simplified in the following way.

$$1 - \cos(\beta h) = 2 \sin^2(\beta h/2)$$

and

$$\sin(\beta h) = 2 \sin(\beta h/2) \cos(\beta h/2)$$

Using these identities,

$$V_{oc} = \frac{E_o}{\beta} \tan(\beta h / 2) \quad V \qquad \textbf{Eq. A-5}$$

Now, if $\beta h/2 << 1$, $\tan(\beta h/2) \approx \beta h/2$ then $V_{oc} \approx E_o h/2$ volts. This final result is the well known result for the voltage induced across the terminals of an electrically short dipole antenna [A2].

It might also be noted that when $\beta h/2 = n\pi/2$, the open circuit voltage apparently becomes infinite. This, however, is not a violation of the laws of physics, because the input impedance (as will be seen in the next section) also becomes infinite under these same conditions and the energy that can be absorbed from the antenna is finite.

The input impedance can be determined by placing a source at the terminals (like a transmitting antenna). For this, it is necessary to have the near field of a linear, sinusoidal current. Using this, we find,

$$Z_{in} \cong \frac{j60}{\sin^2(\beta h)} \int_0^h \sin[\beta(H - z)] \left[\frac{e^{-j\beta R_1}}{R_1} + \frac{e^{-j\beta R_2}}{R_2} - 2\cos(\beta H) \frac{e^{-j\beta r}}{r} \right] dz \, \Omega \qquad \textbf{Eq. A-6}$$

After integration the impedance can be expressed as

$$Z_{in} = R_{r(base)} + jX_{(base)} \ \Omega. \qquad \textbf{Eq. A-7}$$

Note that the subscript "base" means that the equation uses the voltage and current at the open circuited terminals or "base" as required.

The real part is

$$R_{r(base)} = \frac{1}{\sin^2(\beta h)} \{15[(2 + 2\cos(2\beta h)) S_1(2\beta h) - \cos(2\beta h) S_1(4\beta h)] - 2\sin(2\beta h) S_i(2\beta h) + \sin(2\beta h) S_i(4\beta h)\} \quad \Omega \qquad \textbf{Eq. A-8}$$

where

$$S_1(x) = \int_0^x \frac{1-\cos(v)}{v} dv, \qquad S_i(x) = \int_0^x \frac{\sin(v)}{v} dv$$

are an alternative basic sine integral and the sine integral respectively.

The imaginary part is

$$X_{(base)} = \frac{-30}{\sin^2(\beta h)} \left\{ \sin(\beta h)\cos(\beta h)\left[2C_i(\beta h) - 2C_i\left(\beta a^2/2h\right) - C_i(4\beta h)\right] - \frac{\cos(2\beta h)}{2}\left[2S_i(2\beta h) - S_i(4\beta h)\right] - S_i(4\beta h) \right\} \quad \Omega \qquad \textbf{Eq. A-9}$$

where

$$C_i(x) = -\int_x^\infty \frac{\cos(v)}{v} dv$$

is the cosine integral

Using series expansions for small arguments and asymptotic curve fitting for moderate and large arguments, the special functions and be evaluated and the current calculated [A3].

Quasi Static Approximation

As mentioned above, if $\beta h/2 << 1$, $\tan(\beta h/2) \approx \beta h/2$ and

$$V_{oc} \approx E_{oh}/2. \qquad \textbf{Eq. A-10}$$

Similarly, if $\beta H/2 << 1$, the Thevenin impedance can be written as

$$Z_{th} \approx -jX = \frac{-j}{\omega C}\,\Omega \quad \text{where} \quad C \approx \frac{\pi\varepsilon_o h}{\ln\left(\frac{\sqrt{2}h}{a}\right)} \quad F \qquad \textbf{Eq. A-11}$$

where C is the self capacitance of the mast.

References

A1. Weeks, W. L. Antenna Engineering, McGraw-Hill Book Company, New York, 1968

A2. Jordan, E. C., Electromagnetic Waves and Radiating Systems, Prentice Hall, New York, 1950

A3. Abramowitz, M and L. A. Stegun, Handbook of Mathematical Functions, US Department of Commerce, National Bureau of Standards, Washington DC, 1964

B
ANALYTIC THEVENIN IMPEDANCE MODEL FOR THE HORIZONTAL FENCE

The purpose of this derivation is to illustrate how an analytic closed form model for the Thevenin equivalent circuit of a horizontal fence over a perfect ground illuminated by a vertically polarized plane wave can be derived. This model is useful because it is relatively simple and can be used quickly to evaluate the effect of various parameters.

Using image theory, the problem illustrated in Fig. 7-4 can be simplified as shown in Fig. B1.

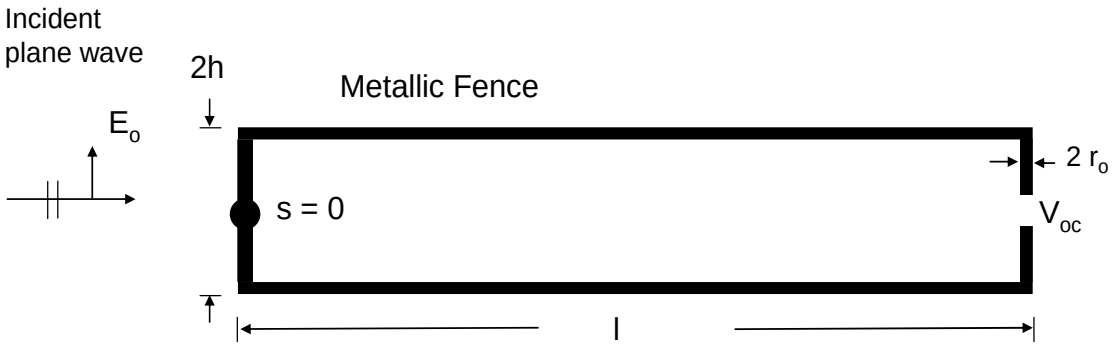

Figure B-1
Image theory equivalent.

A Thevenin equivalent model for this system can be developed using Eq. A1. The current induced on this fence when it is driven by a source at its terminals can be approximated by the transmission line approximation for a short circuited line as long as $l >> h$. If better accuracy is needed, it is possible to use a numerical program such as MININEC to calculate this current. This transmission line current can be written as

$$I_t(s) = I_m \cos(\beta s) \qquad \textbf{Eq. B-1}$$

where s is the distance measured from the point of symmetry opposite the terminals. As shown in Fig. B1. Note here that the "ends" of the fence have been included in the length of the system so that

$$I_{in} = I_t(2h+l) = I_m \cos(\beta(2h+l)) \qquad \textbf{Eq. B-2}$$

Given this and the fact that the electric field is vertically polarized, the only parts of the fence that contribute to V_{oc} are the ends. Hence

$$V_{oc} = \frac{2E_o}{\beta \cos[\beta(2H+l)]}\left\{\sin(\beta H) - e^{-j\beta l}\left[\sin[\beta(2h+l)]\right] - \sin[\beta(h+l)]\right\} \qquad \textbf{Eq. B-3}$$

Using first order small argument expansions for the trigonometric functions that are valid for βl, βh << 1 and the fact that $E_o = B_o\eta_o/\mu_o$ for a plane wave,

$$V_{oc} \approx j\omega 2B_o lh \qquad \textbf{Eq. B-4}$$

This is what would be calculated from an elementary application of Faraday's law to a loop with uniform current on it.

The Input impedance can also be approximated using transmission line theory for a short circuited open wire transmission line so that

$$Z_{in} \approx jZ_o \tan(\beta(2h+l)) \qquad \textbf{Eq. B-5}$$

Where $Z_o = 120 \ln(2h/r_o)$ is the characteristic impedance of a parallel wire transmission line.

The error in making this approximation can be determined by comparing the input impedance from Eq. B5 to that calculated by using MININEC. This is shown in Fig. B2 below.

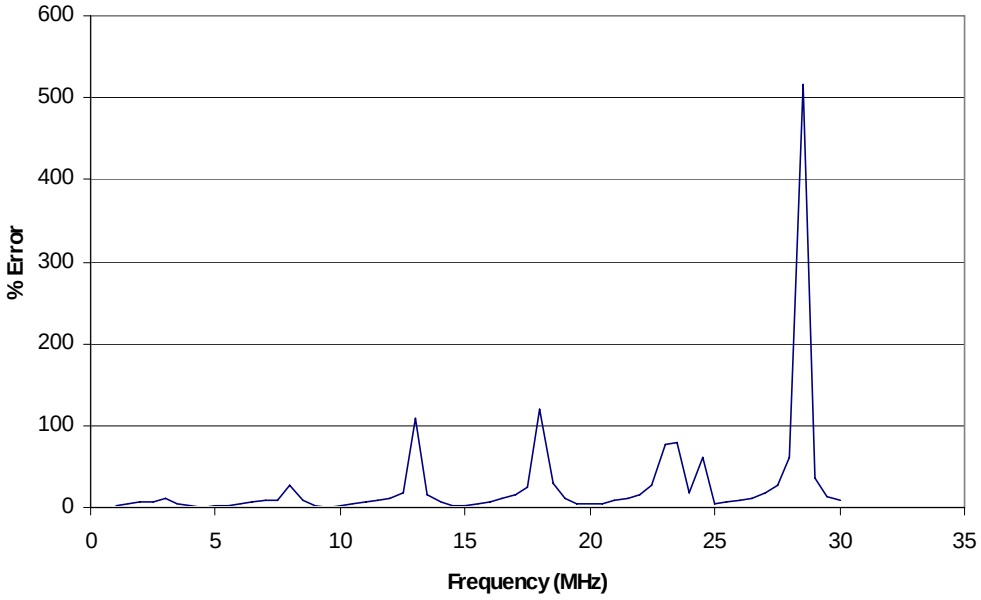

Figure B-2
Percentage error incurred by using the transmission line approximation for the fence current.

It is clear that (aside from a few frequencies) that the error is small and the results generally useful up to 20 MHz.

Quasi Static Approximation

As mentioned above, if $\beta h/2 << 1$,

$$V_{oc} \approx j\omega 2B_o lh. \qquad \textbf{Eq. B-6}$$

Similarly, if $\beta(2h + l) << 1$, the Thevenin impedance can be written as

$$Z_{th} \approx j\omega L(2h + l) \qquad \textbf{Eq. B-7}$$

where L is the inductance per unit length of the fence. Thus, the Thevenin impedance is inductive as expected. Clearly, this impedance is quite low at low frequencies and the impedance of the person dominates.

C
CHARACTERISTICS OF RF BURNS

The US Naval Safety Center has described an RF burn as the result of RF current flow through that portion of the body in direct contact with a conductive object (in which an RF voltage has been induced) or at the site of a spark discharge (no direct contact with a conductive object). In a more practical sense, the term RF burn normally implies an almost instantaneous burning of the skin by a momentary electrical arc of RF energy. Actual physical contact with a conductor energized with RF energy can obviously lead to localized heating of tissue if the resulting local current density is sufficient with the result being an RF burn. But, the more hazardous case is generally that of when the voltage difference between the body and an object being touched is sufficient to cause an arc.

RF burns can exhibit different appearances depending on the magnitude of the current density, its spatial distribution, and the duration of the current flow. In many instances, because electrical arcs are normally startling and painful to the individual receiving the arc, there is a tendency to quickly withdraw from the situation that led to the arc. This often leads to an RF burn that similar to an abrasion of the skin over some region. An example is an individual brushing against a guy wire at an AM radio broadcast station with a series of arcs that "dance" across the skin's surface, leaving a superficial scorching of the skin, typically removing the outer most epidermal layer. The extent of the burn is related to the amount of skin surface that is maintained at just the correct distance from the wire to sustain the arc phenomenon for some limited period of time. An RF burn will occur anytime that an arc exists between the skin surface and an energized object.

Figure C-1
Superficial RF burn showing both the primary injury site an adjacent white singed area.

A classical superficial RF burn is illustrated in Figure C1 that shows a primary injury site with an adjacent singed area of white tissue, somewhat similar to the white burn marks that cigarette smokers sometimes experience in handling a cigarette. A much more serious RF burn is shown in Figure C2 in which the foot of a man has been charred from a large arc incurred while attempting to dismount a high power AM radio station antenna tower. While still holding to the tower, one foot was allowed to touch the ground and just prior to contact the high voltage at the base of the tower resulted in a significant arc with substantial tissue damage.

Figure C-2
Serious, large area RF burn to foot of individual dismounting a high power AM radio station antenna tower [C1]

RF burns share a property with the operation of electro-surgical units (ESUs) used in hospital operating rooms. ESUs use high RF voltages to cut tissue by creating extremely intense current densities in the tissue, typically through the process of tiny electrical arcs between the end of an electrode and the tissue. A shower of sparks is concentrated in a small area leading to almost instantaneous evaporation of the water in tissue cells achieving special surgical effects namely cutting, coagulation and desiccation. RF burns are commonly described as deep within the tissue and slow to heal. This has been ascribed to the "sealing" action afforded by the coagulation effect that can occur at subsurface points along the tissue cutting plane. When the burn is caused by random sparks, small pin-hole burns can happen.

Generally, RF burns are treated like conventional thermal burns but the burns should heal from the interior and the searing characteristic of the burn process can inhibit this process. RF burns should be provided proper medical attention, including the small pin-hole type burns. Petrolatum gauze can be used to cover RF burns temporarily before treatment by a physician [C2]

The most effective means for mitigating RF burns is via the use of gloves. Gloves introduce an impedance that depends on the particular material that the glove is made of, the degree of wetness as a result of perspiration, and the pressure used in gripping an object. A variety of work gloves have been evaluated for their ability to reduce RF current flow [C3]. However, if the RF voltage that exists between the hand and the object being grasped is sufficiently high, an

arc can still exist and result in a potential hazard. Table C1 illustrates measured current reduction factors found for a range of different gloves subject to AM radio broadcast frequencies. For these tests, the voltages were low enough that arcing did not occur.

Table C-1
RF current reduction factors for various work gloves [C3]. The designations A-C refer to different types of work gloves. The designations do not refer to any physical parameter such as glove thickness. Details can be found in [C3].

Summary of Glove Current Reduction Tests in the AM Broadcast Band									
Current Reduction Factors for Low, Medium and High Grasping Pressure									
	F = 0.55 MHz			F = 1.0 MHz			F = 1.6 MHz		
Glove	High	Med	Low	High	Med	Low	High	Med	Low
A	8.9	10	15	5.9	8.9	9.3	4.2	4.7	5.7
B	11	12	17	6.7	8.9	9.4	4.9	5.7	6.1
B	12	14	19	6.8	10	11	4.7	6.1	7.6
C	26	28	31	20	23	27	8.5	9.7	13
Rubber	6.0	7.5	9.3	4.0	5.3	6.7	2.8	3.3	3.8
Rubber + B	15	18	23	9.4	11	12	6.1	7.3	8.4

The influence of grip pressure is illustrated in Figure C3. More specifically, as the grasping pressure is increased, more current flows through the glove (i.e., a smaller current reduction factor). Figure C3 also illustrates an important aspect of contact current mitigation when gloves are used in higher frequency environments. The curve shows the general trend of less current reduction with increasing frequency. This can be viewed as the result of less capacitive reactance at higher frequencies. Figure C4 shows the use of a conventional leather palmed-canvas backed work glove for grasping a guy wire at a multi-transmitter VHF/UHF broadcast site (no AM radio broadcasting present). In agreement with the higher frequency trend in Fig. C4, the glove was found to offer essentially no reduction in the measured contact current compared to a bare-handed gripping of the wire. This is presumably because of the relatively low capacitive reactance offered by the glove at the higher frequencies associated with the broadcast site. This test suggested that work gloves used at VHF/UHF transmitter sites, may provide little if any protection against reducing contact currents.

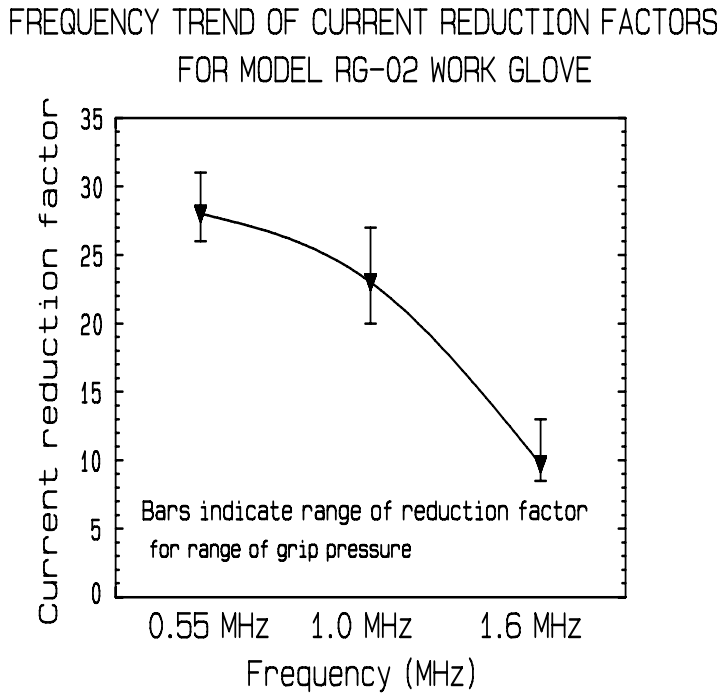

Figure C-3
Influence of grip pressure on RF current reduction factor for gloves. The top and bottom of the bars represent the highest and lowest reduction factors for the lowest and highest grip pressure respectively.

Figure C-4
Evaluating the ability of a leather work glove to reduce contact currents at a VHF/UHF broadcast site found on a tower guy wire. The measured contact current of 92.2 mA (slightly less than the IEEE MPE for contact current in a controlled environment) with the glove was unchanged when the glove was removed and the wire was grasped barehanded.

This same phenomenon is also exhibited by floor mats that are sometimes used to lessen the magnitude of induced body currents when working near equipment that produces strong RF fields such as RF dielectric heat sealers. At higher frequencies, the mitigating effect of insulative floor mats is reduced.

Alerting personnel to the potential for experiencing an RF burn can be an important part of an RF safety program. Safety signage has been produced that is used at transmitter sites wherein strong RF fields exist, particularly at medium wave frequencies. Figure C-5 shows a sign designed to alert individuals of contact currents associated with guy wires that are typically found at broadcast sites that may exceed recommended limits. A common phenomenon is the induction of RF currents on tower guy wires caused by the radiated fields of AM or VHF transmitters. Figure C-6 illustrates a sign intended for placement near the base of AM radio towers where the hazard of RF burns is often greatest. The signal word DANGER is used since the destruction of tissue in an RF burn is deemed a potentially serious injury [C4].

Figure C-5
Caution sign used for alerting personnel to potential for excessive RF contact currents associated with guy wires.

Figure C-6
A danger sign normally used at the base of AM radio towers to alert persons of the potential for an RF burn.

References

C1. Hocking B., Joyner K, Newman H and Aldred R. "Radiofrequency Electric Shock and Burn," Med. J. Aust. 1994:161: 683-685.

C2. http://www.tpub.com/content/istts/14225/css/14225_59.htm.

C3. Tell, R. A. "RF Current Reduction Provided by Work Gloves at AM Radio Broadcast Frequencies." 1993 Technical report prepared for the Federal Communications Commission, Office of Engineering and Technology, Washington, DC, FCC/OET RTA 93-01 [NTIS order no. PB94-117041]).

C4. IEEE, "**IEEE** Recommended Practice for Radio Frequency Safety Programs, 3 kHz to 300 GHz"IEEE Standard C95.7-2005, IEEE, 3 Park Avenue, New York, NY, 10016-5997

D
DESCRIPTION OF THE FDTD METHOD

The FDTD method is a relatively straightforward computational technique for solving Maxwell's equations [D1, D2]. It is used here and will be used in future work because it gives the user a significant amount of freedom to define the geometry of the problem. This is important since in future work, it will be necessary to use a much more anatomically correct model for a human than has been necessary prior to studying RF burns at frequencies approaching and above 100 MHz. Arguably the one major drawback of the technique is that it is computationally expensive. Despite this drawback, its ease of use and its ability to solve problems of great complexity make it the preferred technique in many applications.

Here, the key underpinnings of the FDTD method will be briefly described with the focus being on both the versatility of the method and why it is voracious in terms of computational resources. As the name implies, the FDTD method is a time-domain technique. The fields throughout a given computational domain are assumed to be known at some initial time. Almost invariably the assumption is that these initial fields are simply zero. Then, "update equations" are used to advance the fields forward in time. These update equations express the fields at a specified future time in terms of the known past fields. (As the fields are advanced in time, it is also necessary to introduce some energy into the computational domain. This can be accomplished by embedding a source in the computational domain or by using what is effectively a Huygens surface through which the fields radiate into the domain. These details will not be considered here.)

Here, the steps used to obtain the update equation for one component of the electric field will be described. The update equations for the other field components are obtained in a similar fashion.

Starting with Maxwell's curl equations, i.e., Ampere's and Faraday's Laws, the FDTD method is obtained by discretizing both time and space. Electric fields are assumed to exist at discrete instances of time that are separated by a temporal step Δ_t. The magnetic fields are assumed to exist at instances of time that are offset $\Delta_t/2$ from the times at which the electric fields are given.

In addition to this temporal offset of the fields, all the field components are offset in space as well. Think of space being discretized into small cubes with the cube axes aligned with the x, y and z directions. The cube will be assumed to have sides of $\Delta_x = \Delta_y = \Delta_z = \delta$. (The discretization of space need not be uniform, but is taken as such here merely for the sake of simplicity.) The electric fields can be thought of as existing along the edges of a cube, where the x component of the field E_x is along the x-oriented edges of the cube, E_y is along the y-oriented edges of the cube, and E_z is along the z-oriented edges of the cube. On the other hand, the magnetic fields can be visualized as existing at the center of each face of a cube where each component is oriented normal to that face. Notice that in this arrangement one can think of four electric field components on the edges of a face as swirling around (or surrounding) each magnetic field component. Conversely, by considering the four faces that abut each edge (when one takes into

account neighboring cubes), one can also think of four magnetic field components as swirling around each electric field component.

This discretization gives rise to the "Yee cube" named in honor of Kane Yee who first proposed the FDTD method in 1966 [D1]. The repetition of the cube throughout the volume of interest gives rise to the Yee grid. With the Yee grid in place, the derivatives in Ampere's and Faraday's Laws are replaced with finite differences. As an example, consider Ampere's Law which is given by

$$\varepsilon \frac{\partial E}{\partial t} + \sigma E = \nabla x H. \qquad \textbf{Eq. D-1}$$

Taking only the z component yields

$$\varepsilon \frac{\partial E_z}{\partial t} + \sigma E_z = \frac{\partial H_y}{\partial x} - \frac{\partial H_x}{\partial y} \qquad \textbf{Eq. D-2}$$

In the discretized space the E_z component of the field is assumed to exist at points such that

$$E_z(x, y, z, t) = E_x(m\delta, n\delta, [p+1/2]\delta, q\Delta_t) \quad \text{where} \{m, n, p, q\} \in \text{int eger} \qquad \textbf{Eq. D-3}$$

Within the FDTD grid, the location of the field is completely determined by the three spatial indices {m,n,p} and the temporal index q. It is common practice to write the field in terms of these indices as

$$E_z\Big|^{q}_{m,n,p+1/2} = E_z(m\delta, n\delta, [p+1/2]\delta, q\Delta_t) \qquad \textbf{Eq. D-4}$$

The x and y components of the magnetic field (which are on the faces of the cubes) can be described as existing at

$$H_x\Big|^{q+1/2}_{m,n+1/2,p+1/2} = H_y(m\delta, [n+1/2]\delta, [p+1/2]\delta, [q+1/2]\Delta_t) \qquad \textbf{Eq. D-5}$$

$$H_y\Big|^{q+1/2}_{m,n+1/2,p+1/2} = H_x([m+1/2]\delta, n\delta, [p+1/2]\delta, [q+1/2]\Delta_t) \qquad \textbf{Eq. D-6}$$

Replacing the derivatives in (D2) with finite difference and expanding the equation about the space-time point (mδ, nδ, [p+1/2]δ, [q+1/2]Δ_t) yields

$$\varepsilon \frac{E_z\Big|^{q+1}_{m,n,p+1/2} - E_z\Big|^{q}_{m,n,p+1/2}}{\Delta_t} + \sigma \frac{E_z\Big|^{q+1}_{m,n,p+1/2} + E_z\Big|^{q}_{m,n,p+1/2}}{\Delta_t} = \frac{H_y\Big|^{q+1/2}_{m+1/2,n,p+1/2} - H_y\Big|^{q+1/2}_{m-1/2,n,p+1/2}}{\delta} - \frac{H_x\Big|^{q+1/2}_{m,n+1/2,p+1/2} - H_x\Big|^{q+1/2}_{m,n-1/2,p+1/2}}{\delta} \qquad \textbf{Eq. D-7}$$

Note that the electric field is not available at a time-step of q+1/2 (the electric field is available at integer time steps). Nevertheless, (D7) was obtained by expanding the field about the time-step q+1/2. The temporal derivative (which corresponds to the displacement current) is approximated by a finite difference where the field is advanced or retarded a half step in time, thus giving integer time-steps. However, the undifferentiated term, i.e., σE_z, which represents the conduction current is not differentiated. This term is approximated by averaging (in time) the nearest values of the electric field. From (D7) we can obtain the "update equation" for the E_z component of the electric field. This equation expresses the electric field at time-step q+1 in terms of fields that existed earlier, i.e., either at time q+1/2 or at q. The update equation is given by

$$E_z\Big|_{m,n,p+1/2}^{q+1} = \frac{1-\frac{\sigma\Delta_t}{2\varepsilon}}{1+\frac{\sigma\Delta_t}{2\varepsilon}} E_z\Big|_{m,n,p+1/2}^{q} + \frac{\frac{\Delta_t}{\varepsilon\delta}}{1+\sigma\Delta_t}\left(H_y\Big|_{m+1/2,n,p+1/2}^{q+1/2} - H_y\Big|_{m-1/2,n,p+1/2}^{q+1/2} - H_x\Big|_{m,n+1/2,p+1/2}^{q+1/2} + H_x\Big|_{m,n-1/2,p+1/2}^{q+1/2} - \right) \qquad \textbf{Eq. D-8}$$

There are a few things to note about (D-8). First, the electric field at the "future" time step q+1 depends only on its past value and the value of the neighboring magnetic fields a half time-step in the past. Second, this equation only involves simple algebraic operations. (These two points are important in that they make parallelization of the FDTD method rather trivial.) And, third, the coefficients in these equations depend on the material parameters ε and σ. The material parameters can vary throughout the grid, i.e., it might be more appropriate to write $\varepsilon|_{m,n,p+1/2}$ and $\sigma|_{m,n,p+1/2}$ show that these are functions of space (but are assumed to be constant in time). Similar equations pertain for the other field components.

In an FDTD simulation all the electric field components are updated and then all the magnetic field components (or vice versa—the order of updating is not important). Each set of updates serves to advance the fields only an amount Δ_t in time. This updating is repeated, perhaps tens of thousands of time, until the fields have obtained some desired state (typically they have either returned to zero or, if a harmonic source is used, the fields have obtained steady-state). The discretization of the computational domain typically has to include any physical structure of interest and at least some of the space surrounding that structure. Additionally, the discretization typically has to be such that there are at least ten spatial steps per wavelength at the highest frequency of interest. These requirements give rise to the need for quite a bit of computational horsepower when considering electrically large problems. Fortunately, as mentioned above, the FDTD method is rather trivially parallelizable and hence large problems can easily be tackled using multi-processors clusters.

References

D1 K. S. Yee, “Numerical solution of initial boundary value problems involving Maxwell’s equations in isotropic media,” *IEEE Transactions on Antennas and Propagation*, vol. 14, pp. 302–307, Mar. 1966.

D2 A. Taflove and S. Hagness, *Computational Electrodynamics: The Finite-Difference Time-Domain Method, 3 ed.* Boston, MA: Artech House, 2005.

E
GLOSSARY

Adiabatic Heating. A process in which no heat is transferred to or from the material except by the electric current.

Basic restrictions. Exposure restrictions that are based on established adverse health effects that incorporate appropriate safety factors and are expressed in terms of the *in situ* electric field (3 kHz to 5 MHz) or specific absorption rate (100 kHz to 3 GHz)

Body resistance. Resistance determined from the ratio of voltage applied to current flowing in a human body, neglecting capacitive and inductive effects.

Conductivity, electrical. The scalar or vector quantity which, when multiplied by the electric field strength, yields the conduction current density; it is the reciprocal of resistivity. Expressed in siemens per meter ($S\ m^{-1}$).

Conductivity. The property (σ) of a material that reflects the relative ease with which electric current moves through it. Conductivity is the reciprocal of resistivity (ρ) and both are characteristics of a material rather than a particular specimen; it is defined for isotropic materials in units of Siemens per meter (S/m) and sometimes in mhos per meter ($\mho$/m); like resistance, conductivity is a function of temperature.

Contact current. Current induced in a biological medium via a contacting electrode or other source of current.

Contact voltage. Voltage between a biological medium and an electrode or current source in the absence of direct contact with the body.

De-energized Conductor. A conductor that is not directly connected to a source of electric voltage

Electric field strength. The force (E) on a stationary unit positive charge at a point in an electric field; measured in volt per meter (V/m).

ELF. Extremely low frequency; frequency below 300 Hz.

Electrical Shock. Stimulation of the nerves and possible convulsive contraction of muscles caused by the passage of an electric current through the human or animal body.

Electrically Short Wire. A wire with length that is a small fraction of a wavelength, where the wavelength in free space in meters is 300 divided by the frequency in megahertz.

FDTD. Finite Difference Time Domain numerical method for solving electromagnetic problems

Frequency. The number of sinusoidal cycles completed by electromagnetic waves in 1 second; usually expressed in Hertz (Hz). One megahertz (MHz) is equal to 1,000,000 Hertz.

Inductive Coupling. Transfer of electrical voltage and/or current from one electrical circuit to another through the magnetic field.

GHz. Gigahertz = 1,000,000,000 Hertz (Hz) where Hertz is one sinusoidal cycle per second

kHz. Kilohertz = 1000 Hertz (Hz) where Hertz is one sinusoidal cycle per second

MININEC. A computer program used to solve electromagnetic problems involving wires and lumped circuit elements such as resistors, inductors and capacitors.

Maximum permissible exposure (MPE). The highest rms or peak electric or magnetic field strengths, their squares, or the plane-wave equivalent power densities associated with these fields, or the induced and contact currents to which a person may be exposed without incurring an established adverse health effect and with an acceptable margin of safety. The MPEs are derived or estimated from the basic restrictions (induced electric field, SAR, or power density). If an exposure is proven to be below the basic restrictions, the MPE can be exceeded. MPEs are sometimes called *reference levels*, *derived limits*, or *investigation levels*.

MHz. Megahertz = 1,000,000 Hertz (Hz) where Hertz is one sinusoidal cycle per second

Parasitically Energized Conductors. Conductors that have currents induced on them by exposure to an external electromagnetic field rather than by direct connection to a voltage or current source.

Quasi-Static. A condition under which an electromagnetic can be treated as if the electrostatic and magnetostatic laws apply. Generally this will occur when the dimensions of the system are small compared to the wavelength of the highest frequency of the source.

Radiofrequency (RF). Any frequency at which electromagnetic radiation is useful for telecommunication. *Note:* In this publication, radiofrequency refers to the frequency range 300 Hz -300 GHz.

Resonance. The change in amplitude occurring as the frequency of the wave approaches or coincides with a natural frequency of the medium

Radiofrequency (RF) burn- The localized burning of skin caused by an electrical arc at radio frequencies. RF burns come about when sizeable RF voltage differences exist between the body and an object sufficient to result in an arc between the object and the body. Typically, RF burns are associated with very small electrical arcs when accidentally touching bare element antennas

that are transmitting or when contacting conductive objects in strong RF field environments such as antenna tower guy wires. Empirical assessments of RF burn conditions indicate that when the open circuit RF potential between the object and the body exceeds approximately 140 volts, RF burns may be experienced upon touch.

Rot-mean-square (RMS)- the effective value of, or the value associated with joule heating, of a periodic electromagnetic wave. The RMS value of a wave is obtained by taking the square root of the mean of the squared value of the wave.

Secific absorption rate (SAR). The time derivative of the incremental energy absorbed by (dissipated in) an incremental mass contained in a volume of a given density. SAR is expressed in units of watts per kilogram (or milliwatts per gram, mW/g). Guidelines for human exposure to radio frequency fields are based on SAR thresholds where adverse biological effects may occur. When the human body is exposed to a radio frequency field, the SAR experienced is proportional to the squared value of the electric field strength induced in the body.

Specific heat capacity: The amount of heat necessary to raise the temperature of a unit mass of a substance 1 ºC. The SI unit of specific heat capacity is the Joule per kg per Kelvin (J/kg·K) or Joule per kilogram degree Celsius (J/kg·ºC).

Thevenin Equivalent. An equivalent circuit defined when two terminals of a linear electromagnetic system that are electrically close to each other can be identified. It is possible to replace the remainder of the system with an equivalent voltage in series with an equivalent impedance.

Wavelength- the length of one complete cycle of an electromagnetic wave propagating in space (the speed of light/frequency). The distance is measured in the direction of propagation between a reference point on one wave and the next point that has exactly the same relative phase.

Export Control Restrictions

Access to and use of EPRI Intellectual Property is granted with the specific understanding and requirement that responsibility for ensuring full compliance with all applicable U.S. and foreign export laws and regulations is being undertaken by you and your company. This includes an obligation to ensure that any individual receiving access hereunder who is not a U.S. citizen or permanent U.S. resident is permitted access under applicable U.S. and foreign export laws and regulations. In the event you are uncertain whether you or your company may lawfully obtain access to this EPRI Intellectual Property, you acknowledge that it is your obligation to consult with your company's legal counsel to determine whether this access is lawful. Although EPRI may make available on a case-by-case basis an informal assessment of the applicable U.S. export classification for specific EPRI Intellectual Property, you and your company acknowledge that this assessment is solely for informational purposes and not for reliance purposes. You and your company acknowledge that it is still the obligation of you and your company to make your own assessment of the applicable U.S. export classification and ensure compliance accordingly. You and your company understand and acknowledge your obligations to make a prompt report to EPRI and the appropriate authorities regarding any access to or use of EPRI Intellectual Property hereunder that may be in violation of applicable U.S. or foreign export laws or regulations.

The Electric Power Research Institute (EPRI), with major locations in Palo Alto, California; Charlotte, North Carolina; and Knoxville, Tennessee, was established in 1973 as an independent, nonprofit center for public interest energy and environmental research. EPRI brings together members, participants, the Institute's scientists and engineers, and other leading experts to work collaboratively on solutions to the challenges of electric power. These solutions span nearly every area of electricity generation, delivery, and use, including health, safety, and environment. EPRI's members represent over 90% of the electricity generated in the United States. International participation represents nearly 15% of EPRI's total research, development, and demonstration program.

Together...Shaping the Future of Electricity

Program:

EMF Health Assessment

Occupational Health and Safety

Printed on recycled paper in the United States of America

1015627

Electric Power Research Institute
3420 Hillview Avenue, Palo Alto, California 94304-1338 • PO Box 10412, Palo Alto, California 94303-0813 USA
800.313.3774 • 650.855.2121 • askepri@epri.com • www.epri.com